Journal of Solid State Electrochemistry (2024) 28:3051–3076
https://doi.org/10.1007/s10008-024-05905-7

REVIEW PAPER

"Contemporary neoteric energy materials to enhance efficiency and stability of perovskite solar cells: a review"

Srish Kulkarni[1] · **Smita Gupta**[1] · **Jignasa V. Gohel**[1]

Received: 22 December 2023 / Revised: 5 March 2024 / Accepted: 16 April 2024 / Published online: 29 April 2024

Abstract

Perovskite solar cells (PSCs) have garnered significant interest in recent years due to their high energy conversion efficiency, unique properties, low cost, and simplified fabrication process. However, the reactivity of these devices to external factors such as moisture, water, and UV light presents significant challenges for their commercial viability, potentially compromising their long-term stability and functionality. To overcome these limitations, researchers have focused on two primary strategies: surface passivation and additive engineering. Recent research developments have shown that surface passivation and additive engineering using conducting polymers (CPs), metal-organic framework materials (MOFs), and inorganic additives have significantly improved the operability of perovskite solar cells (PSCs). CPs form resilient interactions with perovskite grains, enhancing film stability through cross-link bonds. MOFs possess a unique network of functional holes that interact with multiple perovskite layers, maintaining morphology and improving interlayer charge transport. Inorganic additives suppress defects at grain boundaries, promoting the formation and growth of perovskite absorbers while providing mechanical protection. These advancements contribute to overcoming the reactivity limitations of PSCs and bring us closer to the commercialization of this technology. The review focuses on the advancements in similar materials, their passivation principles, and the resulting effects on PSC performance. Key aspects covered include the device structure, targeted defects, passivation processes, and synthesis outcomes. By providing a comprehensive overview, the review aims to assist in the selection and synthesis of novel materials.

Keywords Surface passivation · Additive engineering · Conducting polymers · MOFs · Inorganic materials · Stability

Introduction

Hybrid organic-inorganic perovskite solar cells (PSCs) have achieved remarkable efficiency levels, with recent advancements pushing the efficiency up to 25.8% [1–4]. Perovskite solar cells (PSCs) possess distinct intrinsic properties that contribute to their excellent optoelectronic performance. These properties include a high absorption coefficient, tunable band gap, lower exciton binding energies, efficient charge transport over long paths, and significant dielectric constants [5–8]. Furthermore, the ease of fabrication through solution processing and sequential layer deposition contributes to lower production costs for large-scale device manufacturing [6, 9, 10]. Through techno-economic study, perovskite photovoltaic (PV) modules have a low levelized cost of energy (LCOE) of up to 0.05 USD per KWh provided the model lifetime can be increased to 15–20 years [11, 12].

The long-term stability and operability of perovskite solar cells (PSCs) present a major challenge to their commercialization. PSC stability is affected by the reactivity and degradation of the perovskite active layer when exposed to moisture and oxygen in the environment [13, 14]. Furthermore, working temperature and UV luminance have quite an impact on cell performance. Life cycle assessment of the PSC devices indicates lead toxicity after degradation to be a significant environmental challenge. Several intrinsic defects, such as the recombination of charge carrier recombination of uncoordinated lead atoms, deteriorate the optoelectronic performance of modules [14–20]. As a result, strategies to overcome the limitations and significant improvement in PSC performance are required [21].

✉ Jignasa V. Gohel
sjn@ched.svnit.ac.in

[1] Department of Chemical Engineering, Sardar Vallabhbhai National Institute of Technology, Surat 395007, Gujarat, India

PSC performance can be increased through additive engineering and surface passivation strategies [22–30]. Additive engineering is mainly focused on improving the morphological nature of the perovskites. In this, additives, including organic, inorganic, and metal-organic frameworks (MOFs), can be directly added to the perovskite precursor solution. Surface passivation involves the incorporation of interfacial layers within the solar cell structure to improve stability. Passivation can be accomplished in two ways: chemically and physically [31, 32]. Chemical passivation refers to using interfacial species to reduce defect trap states and optimize charge transmission within the perovskite absorber layer. Physical passivation involves the introduction of an interfacial layer near the active perovskite absorber to isolate specific functional groups and enhance the stability of the cell. Photoelectrodes, crucial in solar energy applications, are materials, often semiconductors, that convert light energy into either electrical or chemical energy. They are integral to solar cells, enabling the conversion of sunlight into electricity, and play a key role in processes like water splitting for hydrogen production and environmental applications [33–37].

This review extensively covers approaches for additive engineering and the passivation of imperfections of PSCs using conducting polymers, MOFs, and inorganic additives. This study highlights the progress made by various research groups in minimizing imperfections and addressing carrier recombination challenges in perovskite solar cells. The study also emphasizes the significance of functional group bonding in improving device performance.

Conducting polymers (CPs) for passivation of PSCs

CPs have received much interest due to their economic importance, good environmental stability, electrical conductivity, and superior mechanical and optical properties as represented in Fig. 1 [38, 39]. Organic polymers that transfer energy via metallic or semiconductor activity are called ICPs (intrinsically conducting polymers). The electrical properties of these materials could be adjusted using essential organic syntheses or advanced dispersion techniques compatible with PSC systems [40, 41]. Conductive polymers, commonly referred to as "polymer blacks," are characterized by their linear backbone structure (Fig. 2). Examples of such polymers include polyacetylene, polypyrrole, and polyaniline, as well as their copolymers [42].

The conductivity of conducting polymers arises from several processes. These polymers consist of consecutive sp^2 hybridized carbon centers, with each center possessing one valence electron in a pz orbital. These orbitals are perpendicular to the three sigma bonds formed by the carbon atoms. The Pz orbitals of the carbon centers in CPs combine to form a delocalized set of orbitals that extends across the entire molecule. This delocalization enables the movement

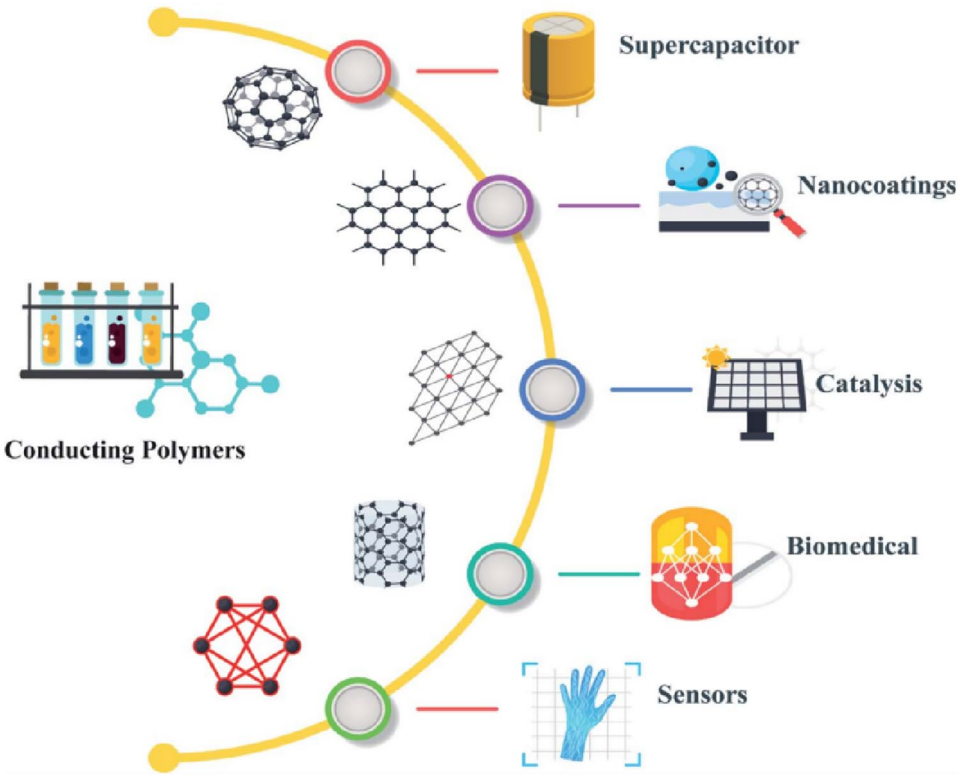

Fig. 1 Conducting polymers and their composites in hybrid perovskite electronics [42]

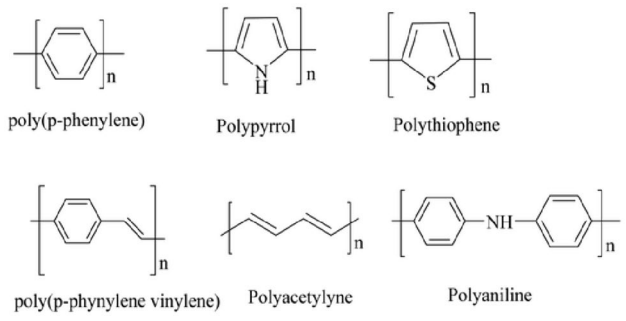

Fig. 2 Structural illustration of different conducting polymers [42]

of electrons throughout the polymer, contributing to its conductivity. When CPs are doped through oxidation, the electrons in the delocalized orbitals experience increased mobility. This doping process involves the removal of some unpaired electrons, leading to improved conductivity by facilitating the movement of charges within the material. The conjugated p-orbitals in CPs form a one-dimensional electronic band. When this band is partially emptied, the electrons within it become highly active. This phenomenon is a result of the unique electronic structure of conducting polymers, which contributes to their distinctive electrical properties. CPs have the ability to establish consistent and predictable interactions with perovskite grains, thereby enhancing the stability of the film. These interactions help to improve the overall stability of the film and mitigate the impact of external factors on the device's performance [43]. The p-conjugated framework present in polymers with double and single bonds plays a crucial role in facilitating enhanced charge transfer. This is achieved through the alteration of functional groups within the polymer structure. By modifying the functional groups, the charge transfer characteristics of the polymer can be optimized, leading to improved conductivity and overall performance [44]. The excellent solubility of CPs in polar solvents helps distribute the precursor solution for uniform interlayer coverage. Indeed, conducting polymers have higher charge transfer which significantly enhances the PSC power conversion efficiency (PCE) when used as charge-transporting layers [45, 46].

Because of their relatively high molecular weights, CPs need not volatilize, which helps them passivate the crystal grain boundaries during perovskite film annealing. Adding polymeric materials increases the grain size and homogenous nucleation, slowing perovskite crystal formation [47–51]. The functional groups on the polymer surface facilitate the formation of a Lewis coordination complex between Pb^{2+} ions and the halide ions of the perovskite material at the crystal surface. This interaction is crucial for enhancing the stability of the perovskite solar cell. As a result, structural imperfections are minimized, with a reduction in localized nonradiative recombination [5, 52–54]. In addition, the hydrophobic functionalization of CPs provides protection to the crystal grains by preventing moisture ingress. This hydrophobicity plays a crucial role by reducing the detrimental effects of moisture on the device. Table 1 depicts the significance of CP additions and their targeted effects. The application of the critical CPs is highlighted in subsequent subsections.

Conducting polymers significantly enhance perovskite solar cells, leveraging their high conductivity for efficient charge transport and improving overall performance. Their hydrophobic nature ensures high resistance to moisture, contributing to the stability of perovskite films. The low solubility, when coupled with chemical modifications, enhances material stability. Overcoming the challenging processability of conducting polymers involves utilizing self-assembly characteristics and scaffold structures. Doping these polymers further improves conductivity, targeting enhanced device efficiency. The unique electrical and optical properties of conducting polymers optimize crystal morphology, crystal growth, and surface passivation, advancing perovskite solar cell technology. Serving as scaffolds for perovskite films, conducting polymers provide structural support, facilitating the formation of high-quality films. Encouraging reactions between PbI_2 and MAI is another contribution, promoting the development of stable perovskite structures. In summary, conducting polymers play a crucial role in improving key aspects of perovskite solar cells, including conductivity, hydrophobicity, solubility, and processability (see Table 1).

Table 1 CPs and their contribution to PSC performance [55]

Material type	Property	Improvement
Conjugated and conductive polymers	1. High conductivity 2. Hydrophobicity 3. Low solubility 4. Challenging processability 5. Conductivity can be improved by doping 6. Solubility can be improved by chemical modification	1. Optimization of crystal morphology 2. Crystal growth effect 3. Surface passivation via electron pair coordination 4. Self-assembly characteristics 5. Scaffold for perovskite film 6. Encourage the reaction between PbI_2 and MAI 7. High resistance to moisture 8. Include unique electrical and optical properties 9. Enhance heat stability

Polyaniline (PANI)

Polyaniline (PANI) is the most promising and investigated CP, with excellent stability, processability, flexible conducting, and optical characteristics. PANI conductivity is highly potent and provides metal-like conductivity at a pH of three [56]. PANI becomes conductive only when tolerably oxidized and behaves as an insulating layer once completely oxidized [57]. Figure 3 shows the different structures of PANI. PANI can be classified into three oxidation states: leucoemeraldine (fully reduced state), emeraldine (intermediate state), and pernigraniline (fully oxidized state). This classification is based on the varying degrees of oxidation that the polymer can undergo, which influences its electrical and optical properties. PANI can also absorb UV-A light wave in its emerald state, protecting PSCs from UV degradation.

Kim et al. [59] incorporated the PANI layer between the electron transfer layer (ETL)/perovskite interface using solution spin coating at precise concentrations. The layer could passivate the interlayer faults while improving the crystalline characteristics of the perovskite layer. Consequently, the UVA light did not reach the interlayer, thereby limiting the Pb^{2+} ions at the interface. In this study, the concentration, thickness, and drying conditions of the PANI passivation layer were carefully controlled and varied as experimental parameters. This allowed for a systematic investigation of the influence of these factors on the performance of the device. By incorporating an interlayer of 65 nm, the PSC achieved a high open-circuit voltage (VOC) of 0.99 V and a power conversion efficiency (PCE) of 15.1%.

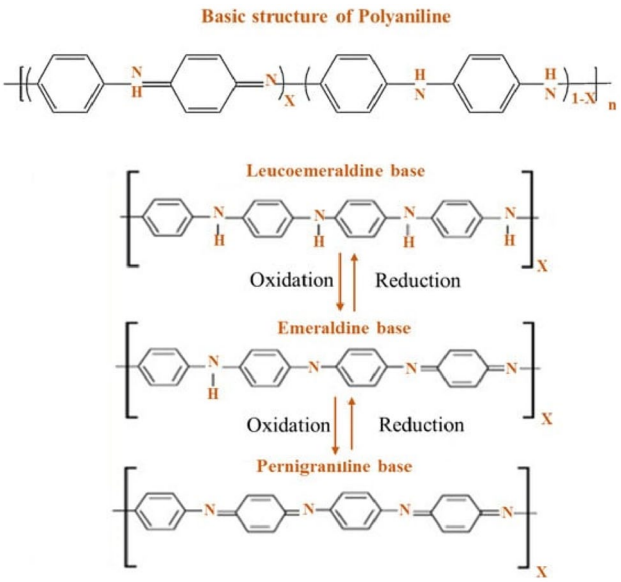

Fig. 3 Structural illustration of different forms of polyaniline [58]

Figure 4 illustrates PANI perovskite devices with better moisture and temperature resistance upon aging tests and the structure of PANI incorporated PSC with its J–V curves having different concentrations of PANI used [59, 60]

Table 2 shows data for improvements in PCE for a specified device structure using PANI as additives. Naji et al. [60] improved the properties of the ZnO-ETL layer by combining ZnO nanoparticles with specific amounts of PANI with the exact device structure as shown in Fig. 4b. The cross-linking served as a bridge between the perovskite granules, reducing carrier accumulation and producing exceptional moisture resistance. The presence of PANI increased the energy barrier for nucleation and growth of the perovskite material. This was achieved by promoting the formation of a Lewis base framework between PANI and the perovskite precursor. The PSC ETL containing 4% PANI (optimum concentration) achieved the highest efficiency, reaching 17.39% as shown in Fig. 4c. This indicates the positive impact of incorporating PANI into the ETL on the overall performance of the solar cell. The treated films indicate substantial enhancement in morphology of the interface.

Zheng et al. [61] implemented PANI as a precursor additive. The quality of the perovskite film exhibited significant improvement, characterized by a refined crystalline structure, enhanced optical absorption, and a uniform surface morphology. These enhancements led to faster photoluminescence (PL) quenching and improved charge transfer within the film. This suggests that the optimized film properties contribute to enhanced performance and efficiency of the perovskite solar cell. The addition of PANI to the device led to a substantial improvement in the PCE, increasing it from 16.96 to 19.09%. Furthermore, the device exhibited reduced hysteresis, indicating improved stability and reliability.

Mei et al. [62] introduced PSCs with PANI as hole transport layer (HTL). Here, bifunctional, economical HTL based on electrochemically formed PANI with dodecyl benzene sulfonic acid was utilized for synergetic modification of the perovskite/HTL interface. The small-area inverted PSC incorporating PANI achieved the highest PCE among PANI-based cells, reaching 20.7%. Moreover, this work included a demonstration of PANI doped with chlorine as an HTL. Chlorine acts as a bridge between the perovskite/PANI interface and significantly improves the optoelectronic properties. The PANI-doped cells in this work were found to obtain higher results compared to earlier research works on PANI passivation.

Abdelmagid et al. [63] reported the synthesis of polyani line:poly(styrenesulfonate) (PANI:PSS) with different PSS doping concentrations. This PANI:PSS material was used as a hole extraction layer in an inverted perovskite device, contributing to its efficient operation. The study found that reducing the content of poly(styrenesulfonate) (PSS) in the polyaniline:poly(styrenesulfonate) (PANI:PSS) composite resulted in increased conductivity of the hole transport layer (HTL). Due to better hole extraction, cells with the

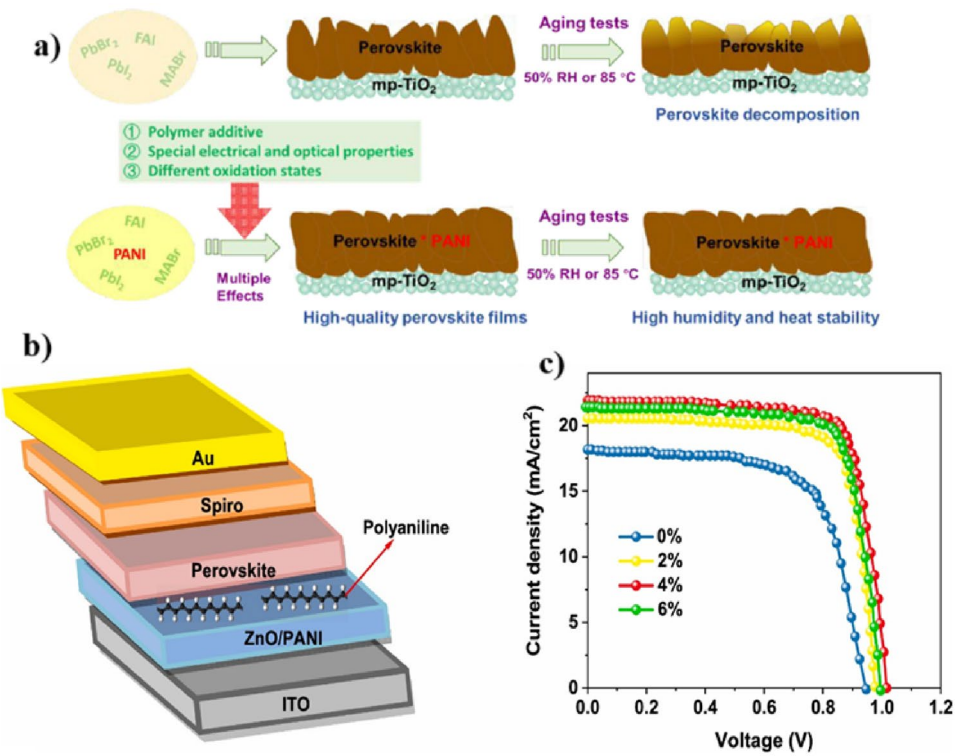

Fig. 4 **a** Schematic process for aging tests of untreated and PANI perovskite films [61]. **b** Schematic representation of the prepared PSC. **c** The J–V tests of the PSCs [60]

highest performance had a short circuit current (Jsc) of 22.5 mA/cm [2], Voc of 0.87 V, fill factor (FF) of 0.42, and PCE of 8.22%.

Lee et al. [64] presented the utilization of camphorsulfonic acid-doped polyaniline (PANI-CSA) as a hole transport layer (HTL) in inverted PSCs. The introduction of PANI-CSA as the HTL aimed to enhance the hole extraction capabilities of the device, thereby improving its overall performance. PANI-CSA, when exposed to m-cresol, acted as a secondary dopant and solvent, facilitating the formation of a highly conductive and uniform film. This effect was attributed to the extension of the chain configuration of PANI-CSA in the presence of m-cresol, resulting in improved film properties. The PANI-CSA-based device achieved a maximum efficiency of 15.42%, while devices with alternative HTLs reached a maximum efficiency of 14.11%. The perovskite/HTL interface significantly increased the device's resistance to moisture exposure.

Lim et al. [65] reported the fabrication of hybrid perovskite solar cells (PSCs) using a water-soluble, self-doped conducting polymer called poly(4-styrenesulfonate)-g-polyaniline (PSS-g-PANI) as a hole extraction layer (HEL). This novel approach aimed to enhance the performance of PSCs by incorporating PSS-g-PANI as an efficient HEL material. The incorporation PSS-g-PANI layer as HEL in the PSCs provided several advantages which included the ability to fabricate the layer at low temperatures using a solution-based method, a high absorption coefficient, and a low energy barrier when integrated with the perovskite layers. The PSS-g-PANI molecules exhibited higher solubility in water compared to traditional PEDOT:PSS molecules. Moreover, they demonstrated good stability over a wide pH range, enabling the fabrication of a HEL with minimal surface defects. PEDOT: PSS-based cell efficiency rose from 7.8 to 12.4% when PSS-g-PANI:PFI was used. This deeper level of energy states reduced the likelihood of charge loss at the interface between PSS-g-PANI:PFI and MAPbI3 in the perovskite solar cells [66]. PSS-g-PANI demonstrated favorable energy level alignment and high transmittance, resulting in improved device properties. Overall, the incorporation of PSS-g-PANI positively influenced the performance of the devices.

Poly(3-hexylthiophene) (P3HT)

Poly(3-hexylthiophene) (P3HT) has garnered significant interest in the field due to its advantageous properties, including high charge transfer capability, ease of fabrication, affordability, improved environmental stability, and conductivity [67–71]. Electron delocalization along this polymer backbone causes electrical conductivity. Apart from their conductivity, these materials exhibit optical properties that align well with the structure of perovskite solar cells (PSCs). They display vibrant colors in response to external stimuli such as solvent changes, temperature variations, applied voltage, and interactions with other molecules. The intriguing interplay between

Table 2 Data for improvements in PCE for a specified device structure using PANI as additives

Sr no.	Additive	Layer	Perovskite	Device structure	PCE (%)	Stability (% retained of initial PCE)	Remarks	References
1	PANI	ETL	$MAPbI_3$	FTO/CP-TiO_2/additive/perovskite/spiro-OMeTAD/Au	10.7 to 15.1%	-	Decrease in non-radiative recombination, confinement of Pb^{+2} ions, enhancement in charge carrier properties	[60]
2	PANI with dodecyl benzene sulfonic acid	HTL	$Cs_{0.05}FA_{0.9}MA_{0.05}PbI_{2.55}Br_{0.4}$	FTO/additive/perovskite/PCBM/C_{60}/BCP/Ag	18.40%	-	Better crystallinity, larger grain size, electronically passivated perovskite via chlorine binding, reduced non-radiative recombination	[62]
3	PANI with ZnO	ETL	$MAPbI_3$	ITO/ZnO/additive/perovskite/spiro-OMeTAD/Au	12.72 to 17.39%	93% for 600 h	Reducing carrier traps, increasing grain size of perovskite layer, lower recombination rate	[60]
4	PANI	ETL	(FAPbI3)0.85(MAPbBr3)0.15	FTO/CP-TiO_2/mp-TiO_2/additive/perovskite/spiro-OMeTAD/Au	16.96 to 19.09%	86% for 1600 h under 50% RH	Improvement in the crystal structure, better moisture and heat resistance, enhanced charge transfer	[61]
5	PANI with camphorsulfonic acid (PANI-CSA)	HTL	$Cs_{0.05}MA_{0.16}FA_{0.79}Pb(I_{0.84}Br_{0.16})_3$	FTO/PEDOT:PSS/additive/perovskite/PCBM/Au	15.42%	70% for 720 h under 40% RH	Improvement in hole extraction, superior photovoltaic performance for flexible substrates	[64]
6	PANI with poly(styrenesulfonate) (PANI:PSS)	HTL	$FA_{0.9}Cs_{0.1}PbI_3$	ITO/PANI:PSS/perovskite/PCBM/Au	7.46 to 11.67%	-	Hole extraction capability increased significantly, enhanced device performance	[63]

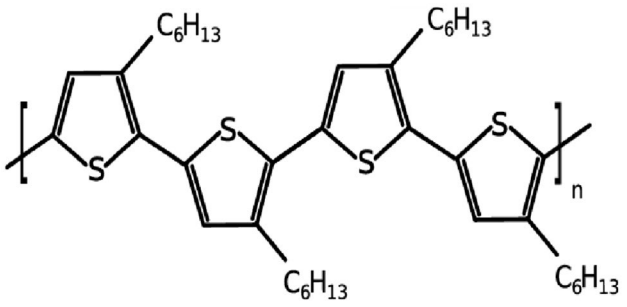

Fig. 5 Structure of P3HT [77]

contorting the polymer backbone and disrupting bond formation is responsible for both the color and conductivity variations observed in these materials. This unique mechanism makes them highly attractive as interlayers that exhibit diverse optical and electrical responses [72–74]. Despite its fundamental differences from the high-performing class of polymers based on the donor acceptor (DA) mechanism, it has demonstrated significant influence in the passivation of PSCs.

Xie et al. [75] used a single additive technique to treat perovskite layers by incorporating P3HT in chlorobenzene (Fig. 5). Adding P3HT improved surface morphology and passivated the perovskite defects, increasing carrier mobility. Moreover, the graded heterojunction formed between perovskite and P3HT resulted in improved hole extraction capabilities, leading to a notable increase in the power conversion efficiency (PCE) from 12.72 to 15.57%. Additionally, the study included a flexible PSC device fabrication, which showed increased PCE from 11.81 to 13.54%. This study successfully developed a high-efficiency carbon-based PSC without the need for a hole transport layer (HTL), by creating a heterojunction structure. SEM (scanning electron microscope) visualizations indicated improved morphological characteristics of perovskite films after treatment. Furthermore, the treatment of perovskite with P3HT resulted in a shift of the valence band energy closer to the work function of carbon, indicating improved alignment at the interface. Incorporating P3HT as an anti-solvent additive improved the energy band alignments of the treated films, which is anticipated to enhance the performance of the devices. In our previous reported work, we developed a perovskite solar cell (PSC) device utilizing P3HT as a gradient heterojunction layer (GHL) at the interface between the perovskite and HTL, as shown in Fig. 6 [76]. The insertion of the GHL at the perovskite interface can passivate uncoordinated Pb^{2+} ions, minimize non-radiative recombination losses, and reduce the hydrophilicity of the perovskite solar cell, resulting in improved device performance. This PSC had a higher PCE than untreated cells, a longer lifetime, and fewer pinholes and imperfections. The work led to an increase in PCE of up to 14.3% compared to 13.2% in pristine samples.

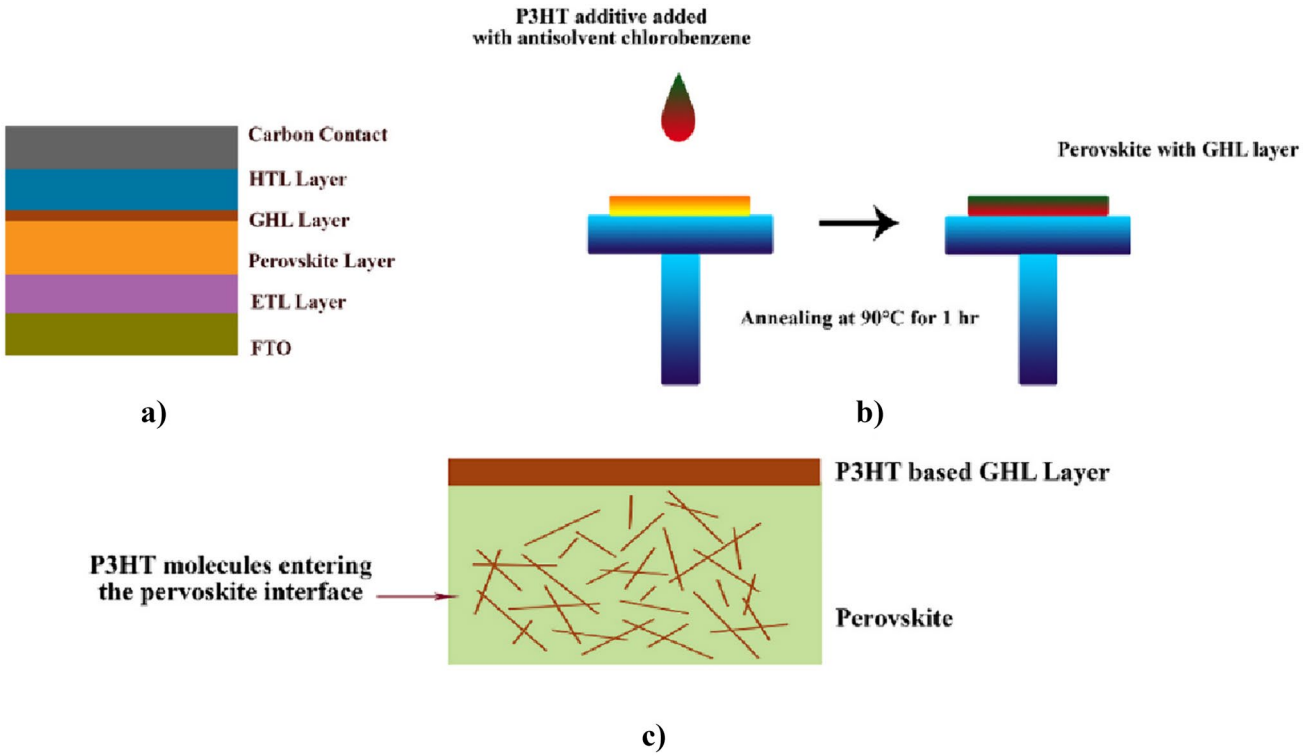

Fig. 6 **a** The structure of PSC, **b** fabrication of P3HT GHL, and **c** the P3HT molecules in grain boundaries at the perovskite/GHL interface [76]

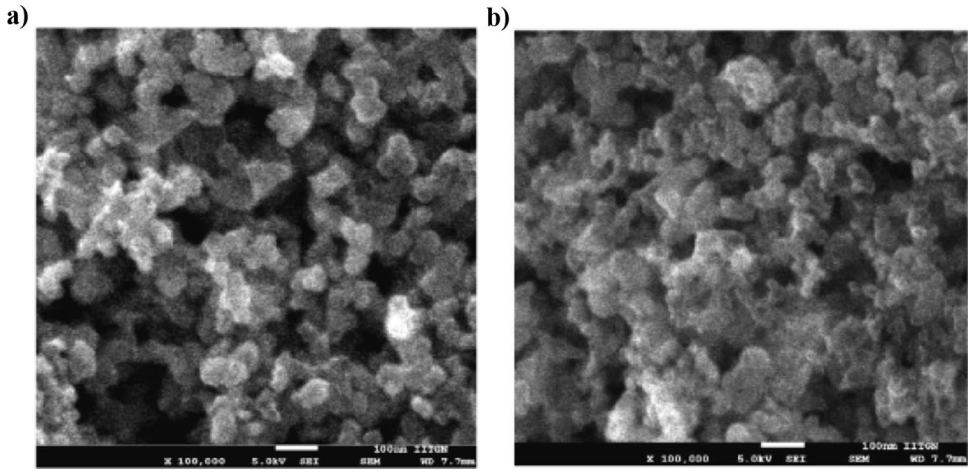

Fig. 7 Field emission scanning electron microscopy of **a** pristine sample and **b** samples with P3HT-based GHL layer [76]

Figure 7 shows FESEM imaging of PSCs with and without GHL. Incorporating the GHL improves the morphology of perovskite. Compared to untreated samples, treated samples had a more homogeneous distribution and fewer pinholes and flaws. Figure 8 shows the contact angle for the devices. The hydrophobic nature of the P3HT molecules in the GHL prevents moisture and water ingress, resulting in a higher contact angle value compared to untreated films.

Jiang et al. [78] employed P3HT with chlorobenzene as an antisolvent for spin coating the perovskite film. P3HT molecules managed to infiltrate along the perovskite crystal structure, filling pinholes and patching up perovskite layer defects. The perovskite valence band (VB) was thus modified to produce a level of energy more aligned with the HTL. As previously demonstrated, the GHL layer containing P3HT and perovskite allows for faster hole migration and increases charge transmission efficiency. The highest-performing solar cell achieved an impressive PCE of 20.0%. Additionally, the incorporation of the hydrophobic mixture layer has improved the stability of the device.

Wang et al. [79] employed P3HT to enhance the $CsPbBr_3$/carbon interlayer in perovskite cells, allowing for greater energy conversion. The results of the systematic analyses demonstrated that the P3HT interlayer could substantially repress charge recombination and improve hole transport ability. As a result, the device achieved a 27% improvement in PCE over the untreated device.

Hybrid poly(3,4-ethylene-dioxythiophene) polystyrene sulfonate (PEDOT:PSS)

PEDOT:PSS conductive polymers have gained significant interest due to their high conductivity, optical transparency, ease of production, and biocompatibility. It is a two ionomer polymer combination. Polystyrene sulfonate, a sulfonated polystyrene carrying a negative charge, is one component of this mixture. The other component PEDOT is a polythiophene-based cross-linked polymer that transports net positive charge. The charged macromolecules combine to generate a macromolecular salt [80]. PEDOT:PSS stands out as one of the most efficient conductive organic materials. Despite having less electrical mobility than silicon, it can be used in PSC devices via stress-relief structures and is sufficiently flexible. Low-cost processing, such as roll-to-roll processing, is feasible with PEDOT:PSS [81]. PEDOT:PSS is extensively employed as a HTL in PSCs because of its excellent hole selectivity along with zwitterionic nature, which allows for solution-based multilayer deposition

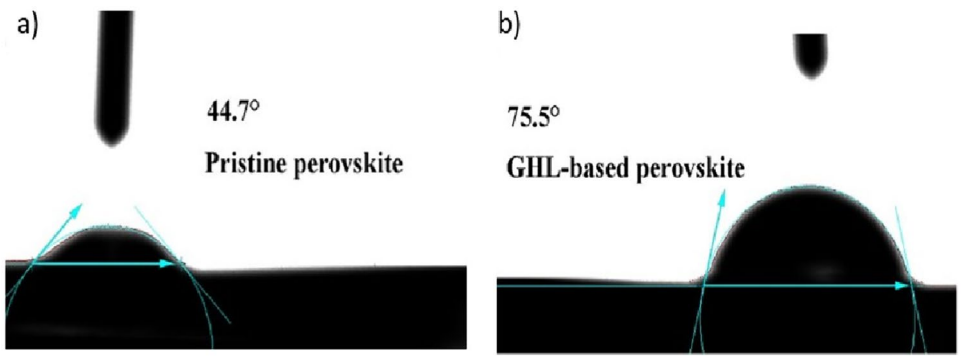

Fig. 8 Contact angle for **a** P3HT GHL and **b** pristine film [76]

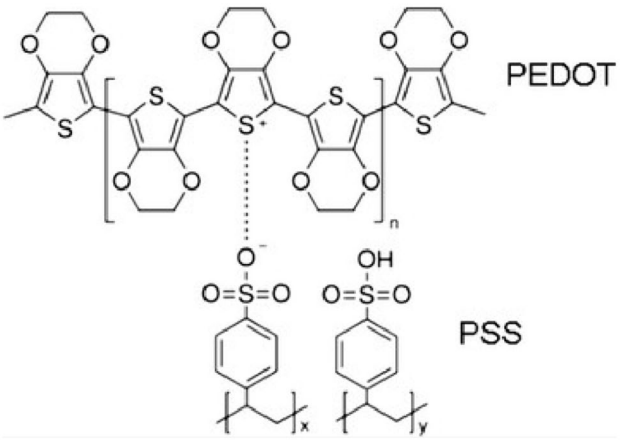

Fig. 9 The chemical structure of PEDOT:PSS [84]

[82]. One of the most significant drawbacks of PEDOT:PSS is open circuit voltage losses caused by incorrect chemical interaction with perovskites. Moreover, energy level mismatch leads to losses in PCE.

Qi et al. [83] investigated the use of three different polymer isoforms of PANI, namely, PANI-carbazole, PANI-phenoxazine, and PANI-phenothiazine, to modify the interface between perovskite and PEDOT:PSS (Fig. 9) as the HTL. The device energy alignment after treatment indicates a wider bandgap to improve the overall performance of the PSC. This resulted in an increase in the absorbance of the film. Moreover, the morphology of the films showed significant uniformity and crystallinity. Modified MAPbI3 PSCs had an increased Voc and an improved PCE of 21.06%.

Wu et al. [85] introduced potassium citrate into the PEDOT:PSS film, resulting in a significant enhancement of the photoluminescence (PL) intensity and confirming effective passivation. The I^- coordinated with the Pb^{2+} at the perovskite layer, improving the contact. The citrate group could confine the residual Pb^{2+} for passivation, while the free I^- was collected back by K^+. In this study, device performance is enhanced from 16.31 to 19.66%. The improvement was due to the modification of the interface caused by the complex formations of the K^+ and citrate groups.

Wang et al. [86] introduced a poly(triaryl amine) PTAA layer between perovskite and PEDOT:PSS HTL to suppress charge recombination and speed up hole transfer. With an optimum content of 0.75 mg/ml of the PTAA layer, a PCE of 19.04% could be achieved. The optoelectronic characteristics and stability of the PSC system have also improved dramatically compared to previous works. The energy band alignment improved the transit of holes from the perovskite film to the PEDOT:PSS layer while avoiding recombination at the interfaces. Moreover, an increase in contact angle (47.1°) was observed for treated cells compared to untreated cells (4.6°).

Zhou et al. [87] presented a novel synergistic strategy for creating stable inverted PSC using PEDOT:PSS HTL, which had better conductivity, lower electrode work function, and excellent morphology. Furthermore, S-acetylthiocholine chloride was used instead of the more expensive PCBM ([6, 6] -phenyl-C61-butyric acid methyl ester) as a passivation layer. Effective passivation of surface charge defects on the perovskite film was observed. This comprehensive approach prolongs the recombination lifetime and lowers the charge trap density. Passivated devices outperformed PCBM in terms of environmental and thermal stability. Consequently, the best cell had an efficiency of 20.06%, while the untreated cell had an efficiency of 18.77%.

The preceding research established that conducting polymers (CPs) are viable passivating additives for PSCs because of their outstanding electrical and ionic conductivity, high stability, and ability to interface with perovskite materials [88, 89]. CPs can operate as a layer of protection, preventing moisture, oxygen, and other contaminants from entering the PSCs. They can also improve the electrical contact between the interlayers, potentially increasing device performance. However, more research is required to enhance deposition processes and comprehend the underlying mechanisms of the passivation process. The following section discusses the significance of metal-organic framework materials (MOFs) in PSC fabrication and the significant advancements reported.

Metal-organic frameworks (MOFs) for passivation of PSCs

Nanoscale metal-organic framework (MOF) compounds possess unique physical and chemical properties applicable in various fields such as magnetism, fluorescence, nonlinear optics, adsorption, separation, catalysis, and hydrogen storage [88, 90–94]. As shown in Fig. 10, MOFs are porous, hybrid materials composed of metal ions coordinated with organic ligands, resulting in a three-dimensional structure. Functionalized

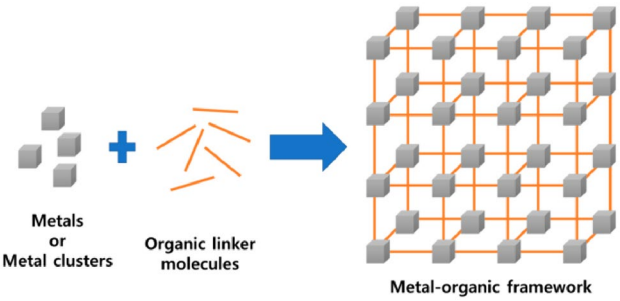

Fig. 10 Schematic of the metal organic framework (MOF) structure [98]

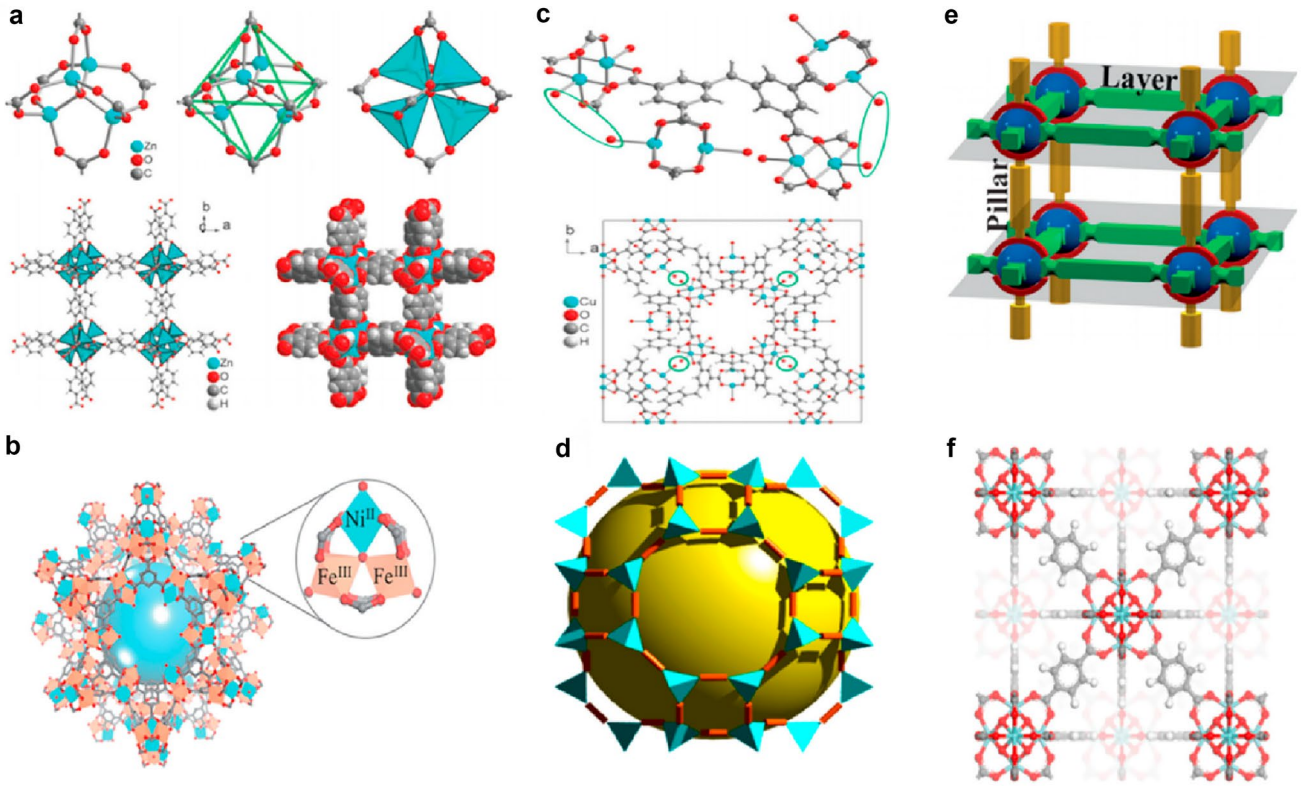

Fig. 11 Schematic structures of MOFs. **a** IRMOF-1 based on 3D-[$Zn_4O(bdc)_3$] compound. **b** MIL-100 based on Fe and Ni. **c** PCN-12 based on Cu **d** ZIF-71 based on Zn. **e** CPLs-55 based on Zn **f** UiO-66 based on Zr [105]

MOFs can be tailored for specific applications through ligand modifications, functional group adjustments, and metal ion doping. These modifications enhance properties, such as increased surface area, accessible pore structure, adjustable pore diameters, and a higher density of active metal sites. As a result, MOFs exhibit superior molecule transport capabilities compared to other porous materials [89, 95–97].

Perovskite absorber layers are sensitive to factors like humidity, temperature, pressure, light, electric field, and chemical environment, which can affect their stability and performance. The degradation of perovskite materials is directly linked to their instability, both functionally and physically. In this sense, including MOFs in perovskite structures by additive engineering can considerably improve the commercialization prospect for PSCs. They are identified according to different groups based on their crystal structure: IRMOFs [99], MILs [100], PCNs [101], ZIFs [102], UIOs [103, 104], and more. Figure 11 shows the three-dimensional structure of various MOF groups.

According to reports, MOFs are used in PSCs in the following ways: (a) incorporated into the ETL, (b) incorporated into the HTL, (c) Added to perovskite precursor, and (d) for interfacial modification.

The ETL plays a crucial role in PSCs by facilitating electron transport and blocking holes. Titanium dioxide (TiO_2) is a commonly employed ETL in PSCs due to its favorable electronic properties, suitable energy gap, transparency, and cost-effectiveness. However, TiO_2 does have some limitations, including low conductivity and the presence of defects such as oxygen vacancies and metal interstitials at surface [106]. Incorporating MOFs here would improve the porosity of the ETL and make it more conducive for charge transfer operations.

The HTL is critical in encouraging electron separation, modifying charge carrier motion and recombination and perovskite crystallization, and establishing ohmic contact at the back contact electrode. At present, 2,2′,7, 7′-tetrakis- (N, N-di-4-methoxyphenylamino)-9,9′-spirobifluorene (spiro-OMeTAD) is the widely utilized HTL for its excellent stability and an acceptable level of energy. However, the lower intrinsic charge mobility may impose limitations on its overall performance [107–109]. The combination of MOF and HTL can enhance the oxidation of spiro-OMeTAD and facilitate charge transport by optimizing band alignment.

MOF materials have made notable progress in PSC interface engineering by serving as a microporous scaffold to regulate the formation of perovskite layers (Fig. 12). This approach enhances the contact at the ETL/perovskite interface, leading to improved crystallinity and film quality [110].

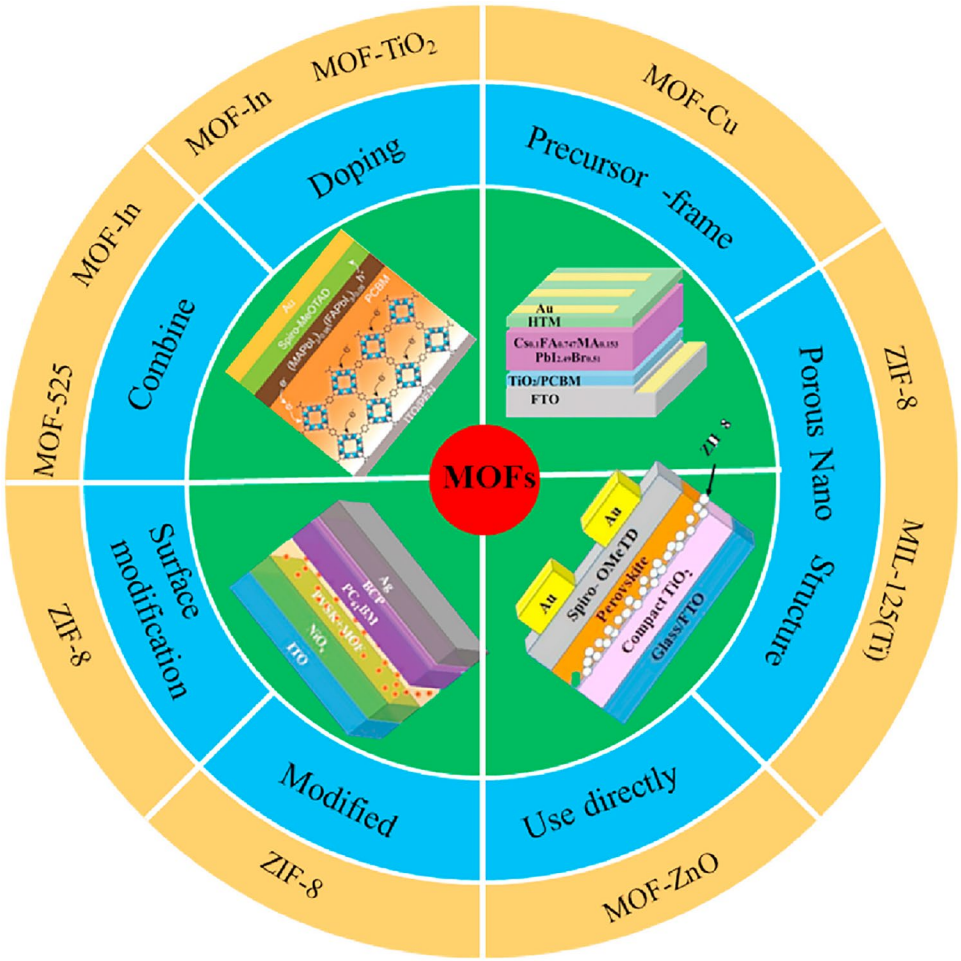

Fig. 12 Various applications of MOFs reported so far [105]

MOFs as ETL modifiers

Table 3 shows standard work recently reported by various researchers on MOFs. Wu et al. [93] used a thiol-complexed conjugated MOF ZrL3 as ETL for an inverted PSC. The MOF demonstrated n-type electron exchange behavior and exhibited an energy level suitable for the ETL/perovskite interface. By preferentially interacting with the carboxyl groups, Zr(iv) ions facilitated the formation of dense, self-supporting thiol arrays that provided steric protection and stabilization around the Zr(iv)-oxo cluster. The abundance of thiol groups on the MOF is especially important as they can form robust networks through chemically bonded disulfide connections, effectively trapping metal ions like lead and tin. By incorporating functionalized MOF materials, a significant amount of Pb^{2+} ions that were lost from damaged perovskite solar cells could be effectively collected and immobilized as water-insoluble solids. This approach not only improved the operational stability of the solar cells but also helped mitigate lead leakage concerns associated with the use of perovskite materials. The incorporation of functionalized MOF materials resulted in a remarkable enhancement in the PCE of the cells, reaching a high value of 22.02%.

Ahmadian-Yazdi et al. [111] utilized zeolitic imidazolate framework-8 (ZIF-8) as an interlayer between the TiO_2 and perovskite (see Table 3). In contrast to the mesoporous TiO_2, ZIF-8 film possessed all the characteristics required to benefit from a more straightforward synthesis process. This layer significantly increased perovskite crystallite size and grain structure. SEM visualization of perovskite films after treatment with ZIF-8 layers indicates larger grain size and better crystal alignment. The MOF addition is supposed to allow homogeneous crystallization of perovskites at layer borders. Additionally, the formation of hydrogen bonds between the methyl group in the ZIF-8 structure and the halide ions of the perovskite structure enhanced the interconnectivity and cohesion among individual perovskite crystals. The treated cell attained PCE of 16.8%, which was adequate compared to previous research groups.

Sadegh et al. [112] employed MOF zinc stannate (ZSO) as an ETL(see Table 3). The fabrication of this layer was achieved using the chemical bath deposition method (CBD). CBD facilitated the formation of a perovskite layer with enhanced surface coverage and larger grain size, leading to reduced recombination losses. The incorporation of MOF at the ETL/perovskite interface improved charge extraction,

Table 3 Data for improvements in PCE for a specified device structure using MOFs as additives

Sr. no.	Additive	Location	Perovskite	Device structure	PCE (%)	Stability (% retained of initial PCE)	Remarks	Reference
1	ZrL3	ETL	$MAPbI_3$	ITO/PTAA/perovskite/PCBM/additive/Ag	22.02	90% for 1000 h at 85 °C	Confinement of Pb^{2+} ions from perovskite layer, shielding and stabilization from the external environment	[93]
2	ZIF-8	ETL	MAI and FA/MA/Cs based mixed cationic	FTO/TiO_2/additive/perovskite/ /Au	16.8		Confinement of Pb^{2+} ions from perovskite layer, Improvement in perovskite crystal structure	[111]
3	Zinc Stannate (Zn_2SnO_4, ZSO)	ETL	FA/MA/Cs based mixed cationic	FTO/ZSO/perovskite/spiro-OMeTAD/Au	21.3	90% for 1000 h	Increase in charge extraction, reduction in trap-assisted recombination	[112]
4	CO-TiO_2 with trimesic acid (H3BTC)	ETL	FA/MA/Pb(I/Cl/Br) mixed cationic	FTO/c-TiO_2/m-TiO_2/additive/perovskite/spiro-OMeTAD/Au	15.75		Suppression of ejecting electrons, higher conductivity of ETL, improved bandgap alignment	[113]
5	PEIE with (Cd3(C6H2TeO4)3·4DMF) MOF	ETL	$FA_{0.25}MA_{0.75}PbI_3$	FTO/additive/perovskite/spiro-OMeTAD/Au	22.22		Increased form and crystalline nature of the perovskite film; faster charge transfer	[114]
6	TiO_2/Al_2O_3/NiO	ETL	$Cs_{0.05}(FA_{0.4}MA_{0.6})_{0.95}PbI_{2.8}Br_{0.2}$	FTO/additive/perovskite-carbon	17	90% for 1020 h at 85 °C (dark conditions)	Increase in bandgap, exciton binding energy, charge carrier lifetime, and diffusion length	[115]
7	Li-TFSI@NH_2-MIL-101	HTL	$MA_{0.14}PbI_{2.55}Br_{0.45}$	FTO/c-TiO_2/$PC_{61}BM$/perovskite/HTL/Au	19.23	85% for 3600 h at 40% RH	Reduction in Li salt, resistance from water, passivation of trap states	[116]
8	HTM-FJU-17	HTL	$MAPbI_3$	FTO/TiO_2/perovskite/HTL/spiro-OMeTAD/Au	20.34	90% for 1000 h	Passivation of organic vacancies, enhancement in hole mobility	[117]
9	Co-NC(HCl)-ZIF-67	HTL-back contact	$MAPbI_3$	FTO/SnO_2/perovskite/additive-back contact	10.72		Suppression of charge recombination, promotion of hole extraction, improvement in perovskite morphology	[118]

Table 3 (continued)

Sr. no.	Additive	Location	Perovskite	Device structure	PCE (%)	Stability (% retained of initial PCE)	Remarks	Reference
10	Core-shell CuO@NiO	HTL	$MAPbI_3$	FTO/c-TiO_2/c-TiO_2/perovskite/additive/Au	10.11	60% for 1920 h	Decrease in defect states, favorable energy alignment, increase in hole mobility and conductivity	[119]
11	$[In_{12}O(OH)_{16}(H2O)_5(btc)_6]_n$ (In-BTC) nanocrystals	HTL	$Cs_{0.05}FA_{0.81}MA_{0.14}PbI_{2.55}Br_{0.45}$	FTO/c-TiO_2/$PC_{61}BM$/	20.87	80% for 288 h at 25 °C	Improved morphology, reduced grain boundaries defects	[120]
12	UiO-66 and UiO-66-NH_2	Precursor	$CH_3NH_3Sn_{0.25}Pb_{0.75}I_3$	FTO/c-TiO_2/m-TiO_2/perovskite/additive/spiro-OMeTAD/Au	15.78		Number of defects reduced, efficient charge transfer	[121]
13	UiO-66	Interlayer	$MAPbI_3$	ITO/NiOx/additive/perovskite/PCBM/Au	17.01	70% for 336 h at 20 °C	Passivation of defects, increase in film robustness, enhanced crystallization	[122]
14	MOF 808				16.55			
15	$Pb(SCN)_2$	ETL	$CH(NH_2)_2SnI_3$	ITO/PEDOT:PSS/perovskite/additive/PCBM/Al	8.40%	-	Uniform grain size, uniform pinholes	[123]

resulting in exceptional photovoltaic performance, reduced hysteresis, and reliable device repeatability. The utilization of modified ZSO ETL in PSCs led to a notable enhancement in efficiency, with a significant increase in open circuit voltage, resulting in a remarkable improvement from 19.3 to 21.3% compared to conventional ZSO-based devices. Contact angle measurement of the PSCs indicated an increase in hydrophobicity in the order of (a) FTO (< 3°), (b) bare ZSO ETL (39°), and (c) CBD-modified ZSO ETL (53°).

Nguyen and Bark [113] successfully prepared doped TiO_2 with trimesic acid (H3BTC) as a MOF (see Table 3). Doping with Co significantly improved the morphological features of the TiO_2 layer that would be employed in the PSC device. After device treatment, the MOF could suppress the excitation and ejecting of electrons, thereby gaining higher conductivity. It boosted device efficiency by up to 15.75% by improving bandgap alignment and decreasing surface layer flaws at the ETL/perovskite interface.

Ji et al. [114] utilized nanofilm of polyethylenimine ethoxylated (PEIE) and tellurophene-based MOF ($Cd_3(C_6H_2TeO_4)_3{\cdot}4DMF$ framework. In this work, the nondestructive passivation of TiO_2 was successful (see Table 3). After modifying the ETL layer, notable adjustments were observed in the shape and crystallinity of the perovskite film, while minimizing the trap states in the TiO_2 layer. These modifications resulted in the successful development of highly efficient and stable PSCs, achieving an impressive power conversion efficiency (PCE) of 22.22%. AFM (atomic force microscopy) and SEM visualizations of the PEIE modification layer along with 2D MOF indicated formation of a giant perovskite crystal, finer crystal lattice, and elimination of the negative effect of PEIE island in the ETL.

Similarly, Liu et al. [115] introduced mesoporous metal oxides $TiO_2/Al_2O_3/NiO$ layered MOF in printable PSCs (see Table 3). The study focused on utilizing a triple cationic perovskite with cesium cation (Cs). Introducing Cs into the perovskite composition, along with the use of MOF, offers several advantages. The partial replacement of formamidinium (FA) and methylammonium (MA) with Cs increases the energy band gap and exciton energy of the perovskite layer. Cesium incorporation also contributes to enhanced carrier longevity and diffusion length, leading to improved charge transport within thick mesoscopic layers. These modifications are instrumental in achieving higher performance and efficiency in perovskite solar cells.

MOFs as HTL modifiers

Wang et al. [116] incorporated novel Li-TFSI MOF (namely, Li-TFSI@NH_2-MIL-101) as HTL for resisting reaction with water molecules (see Table 3). Li-TFSI, present in spiro-OMeTAD to promote hole conductivity, harms device stability. Li-TFSI, owing to its hydrophilic properties, has the ability to transiently convert into a liquid state when exposed to water for a brief period of time. The presence of water or moisture in the environment can lead to uncontrolled oxidation of spiro-OMeTAD, which can negatively impact the reproducibility of the system. Using the MOF reduces the hydrophilicity of the PSC device by increasing the contact angle from 74.53 to 84.60°. The PSCs treated with Li-TFSI@NH_2-MIL-101 achieved a high PCE of 19.01% with a reduced Li salt loading mass. The presence of ammonium groups (-NH_2) in NH_2-MIL-101 enhanced the interaction with uncoordinated Pb^{2+} ions, leading to passivation of trap regions and reduced ion migration at the perovskite/HTL interface. This improved the stability of the devices. Additionally, the incorporation of MOF in the HTL layer improved energy alignment within the device.

Zhang et al. [117] constructed a functional layer HTM-FJU-17 by integrating a capsule of the $(Me_2NH_2)+$ metal-organic framework (FJU-17) into HTM (see Table 3). HTM-FJU-17, with its MOF reticular framework, effectively passivated defects in the perovskite layer by filling organic cation vacancies. The uniform distribution of $(Me_2NH_2)+$ ions within the MOF structure contributed to this passivation process. Furthermore, the MOF anionic framework could stabilize oxidized HTM, increasing hole mobility. The HTM-FJU-17-treated PSCs indicated reduced charge recombination, leading to an improvement in power conversion efficiency (PCE) from 18.32 to 20.34%.

Geng et al. [118] constructed a composite material Co-NC(HCl) fabricated by heating ZIF-67 and etching it with HCl (see Table 3). A series of HTM-free PSC structures were created by combining this paste with conductive carbon (CC). The results show that incorporating the composite interface suppressed charge recombination and promoted hole separation. In the ambient atmosphere, the incorporation of HTM-FJU-17 resulted in a significant improvement in the maximum power conversion efficiency (PCE) of the device, reaching 10.72%. This represents a notable 43% enhancement compared to the untreated device. The enhanced performance of the device can be attributed to the unique morphology of the Co-NC(HCl) composite. Numerous pinholes and flaws were removed from the perovskite boundary in the untreated device after passivation. The shape of the films also improved after utilizing a treated carbon-based counter electrode.

Hazeghi et al. [119] synthesized and employed core-shell CuO@NiO nanoparticles to synthesize HTL (see Table 3). Cu-Ni-BTC nanospheres were successfully synthesized and utilized to create a core-shell CuO@NiO HTL. This hybrid structure combined the benefits of both NiO and CuO inorganic semiconductors, resulting in improved hole mobility and stability. When compared to the NiO HTL, the PSC with the CuO@NiO HTL exhibited a higher conversion efficiency of 10.11%, a significant improvement of approximately 15%. The exceptional performance of the PSC incorporating the core-shell CuO@NiO HTL can be attributed to several factors.

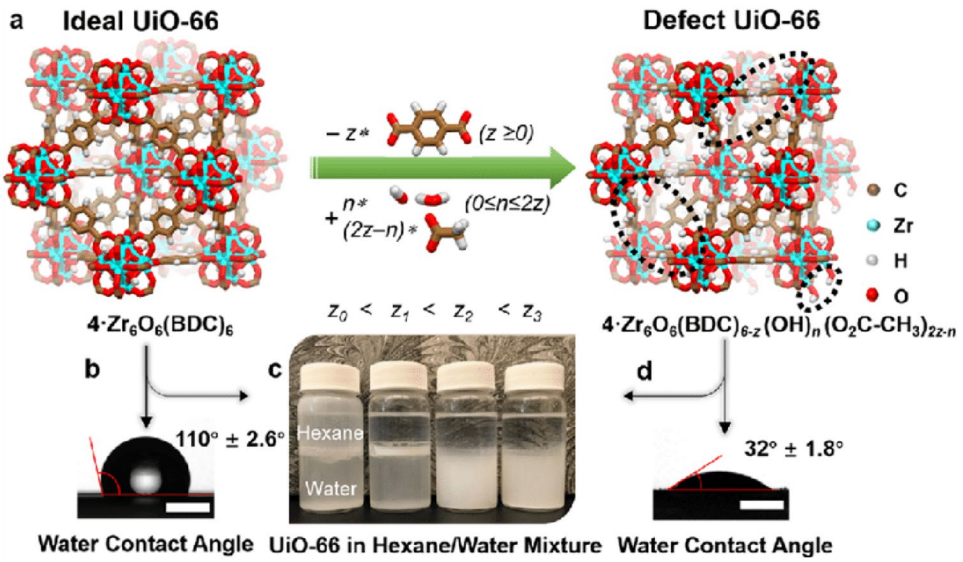

Fig. 13 Schematic of the defect sites and the passivation effect of MOF UiO-66-NH_2 [121]

First, the favorable energy alignment between the HTL and the perovskite layer facilitated efficient charge carrier extraction. Second, the increased conductivity of the CuO@NiO HTL improved charge transport within the device. Additionally, the decreased defect density of the HTL contributed to reduced charge carrier recombination. Experimental studies revealed that the MOF nanoparticles utilized in the core-shell structure exhibited fewer defect states compared to NiO nanoparticles, further enhancing the device performance by minimizing recombination losses.

Zhou et al. [120] incorporated perovskite with indium-based MOF $[In_{12}O(OH)_{16}(H2O)_5(btc)_6]_n$ (In-BTC) heterojunction (see Table 3). The unique interlinked micropores and terminal oxygen sites of In-BTC facilitated the preferential crystallization of perovskite within its regular cavities. This phenomenon led to the formation of perovskite films with improved morphological characteristics and reduced grain defects. The controlled crystallization process within the In-BTC framework resulted in enhanced film quality, contributing to the overall performance and stability of perovskite solar cells. The incorporation of In-BTC into the perovskite solar cell structure led to notable enhancements in interfacial electrical contact, photo-response, and environmental resilience. These improvements translated into a higher fill factor of 0.79 and an elevated power conversion efficiency (PCE) of 20.87% compared to the untreated device. The modified PSC benefited from the superior properties of In-BTC, resulting in improved device performance and stability.

MOFs as interlayer and precursor modifiers

Chang et al. [121] proposed a novel approach to enhance the performance of mixed lead-tin perovskite materials by employing two specific metal-organic frameworks (MOFs), namely, UiO-66 and UiO-66-NH_2 (see Table 3). In contrast to UiO-66, the presence of an electron-donating amine group in UiO-66-NH_2 facilitated interaction with under-coordinated metal cations within the perovskite layer, leading to effective passivation and improved device performance, as depicted in Fig. 13. The precursor solution employed a concentration of 20 mg/ml for the MOF additive.

Interfacial engineering via molecular doping resulted in a high PCE of 13.93% and significantly increased ambient stability. This strategy also applies to low-bandgap (1.3 eV) perovskites, deriving high performance. In contrast to the untreated device deterioration, the PSC containing UiO-66-NH_2 could tolerate more air exposure. SEM analysis revealed that both the treated and untreated devices exhibited similar grain sizes of approximately 400 nm and surface roughness of around 30 nm.

The J–V curves of the PSC are generally showing improved efficiency when MOFs are added as shown in Fig. 14a. This is attributed to the immobilization effect of ZrL3 on leaked Pb^{2+} ions as shown in schematic of the degradation process of PVSCs in Fig. 14b [110]. Similar improvement in efficiency and improved crystalline structure and morphology is also reported by Lee et al. [122], as shown in Fig. 14c–f [123]. It shows the XRD patterns, SEM-EDS, J–V curves, and degradation profile of the pristine perovskite film and the studied hybrid films. Basically, they demonstrated the working of inverted PSCs utilizing perovskite/Zr MOF heterojunction [122]. They investigated the utilization of two chemically stable Zr-MOFs, UiO-66, and MOF-808, as interlayers in perovskite solar cells. The MOFs exhibited the ability to spread throughout the perovskite material, leading to a grain-locking mechanism that enhanced defect passivation and improved the film's resistance to moisture ingress. SEM imaging of both treated and

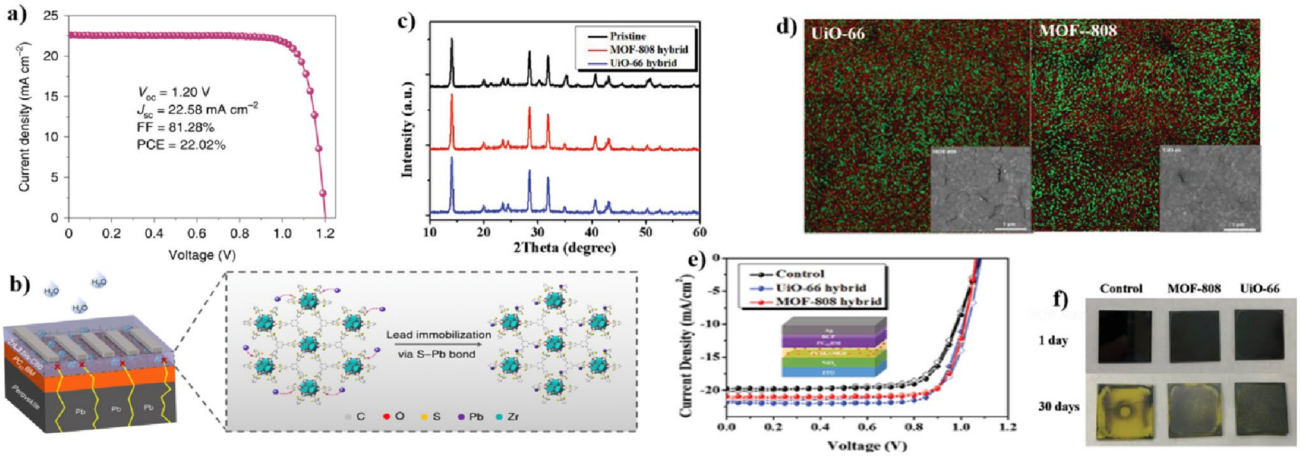

Fig. 14 **a** J–V curve of the champion PVSC with ZrL3. **b** Schematic of the degradation process of PVSCs and the immobilization effect of ZrL3 on leaked Pb^{2+} ions [93]. **c** XRD patterns. **d** The SEM-EDS images (red is I and green is Zr). **e** J–V curves of control, UiO-66, and MOF-808 added PSCs. **f** The real-time images of the hybrid film stored in ambient condition (25 °C and RH: 60 ± 5%) [123]

untreated perovskite solar cell films after aging revealed notable differences (see Fig. 14d). The MOF-treated device exhibited larger perovskite grains, improved lattice structure, and reduced defects compared to the untreated device as shown in Fig. 14c. The 3D porous structure of the MOFs facilitated the incorporation of small perovskite nanocrystals, ensuring the presence of efficient charge-transport pathways across the MOF scaffolds. The superior and enhanced PCE of 17.01% was achieved for UiO-66-modified PSCs, while the MOF-808-modified PSCs achieved an enhanced PCE of 16.55%, surpassing the performance of the untreated device. Additionally, the hybrid film exhibited enhanced ambient stability, addressing one of the key challenges in perovskite solar cell technology.

Essentially, MOFs possess unique properties that make them valuable for numerous applications. In the context of perovskite solar cells (PSCs), several research studies have highlighted the significance of MOFs. By incorporating MOFs as additives, researchers have demonstrated the ability to passivate defects, enhance charge transport, and improve the overall functionality of PSCs. MOFs and MOF-derived materials can be used at various locations in PSCs to improve the layer properties. Furthermore, they are appealing materials for PSCs because bandgaps can be easily adjusted by changing the components by solution synthesis. Essentially, their porous structures can act as protective barriers, improving stability by shielding perovskite layers from environmental factors. MOFs with scaffold structures facilitate controlled perovskite film growth, ensuring uniformity and enhanced device efficiency. Additionally, MOFs contribute to improved charge transport properties, reducing carrier recombination and optimizing overall conductivity. Their selective gas permeability can prevent the ingress of detrimental gases. Tailored optical properties of MOFs complement perovskite materials, enhancing light absorption and spectral response. Furthermore, MOFs can serve as nucleation sites, encouraging controlled perovskite crystal formation. The integration of MOFs thus addresses key challenges in perovskite solar cells, promising advances in stability, efficiency, and overall performance. Thus, MOFs have a tremendous potential to address the device stability issue to popularize and further commercialize third-generation solar cells, and further research is required to study such improvements.

Inorganic additives for passivation of PSCs

Polycrystalline perovskite absorbers commonly exhibit surface and grain boundary imperfections, which can adversely impact the performance of PSCs. These imperfections, depicted in Fig. 14, include impurities, interstitial vacancies, and undercoordinated ions. They act as nonradiative recombination sites, leading to a decrease in overall PSC performance. Additionally, these defects can affect the morphology of the perovskite crystals and the absorption capacity of each layer within the PSC structure (Fig. 15). It is crucial to address and mitigate these defects to improve the efficiency and stability of PSCs. As a result, much work has been carried out on organic compounds like acid base adducts [124–130], polymers [23, 131–134], fullerene derivatives [135–137], organic solvents [138–140], organic halides, ionic liquids [141–145], and graphene and derivatives [138].

The chemical passivation of perovskite crystal surfaces using organic compounds is typically susceptible to degradation when exposed to various stressors, including UV light, temperature, and humidity. This fragility limits their long-term stability in PSCs. Moreover, organic materials may not

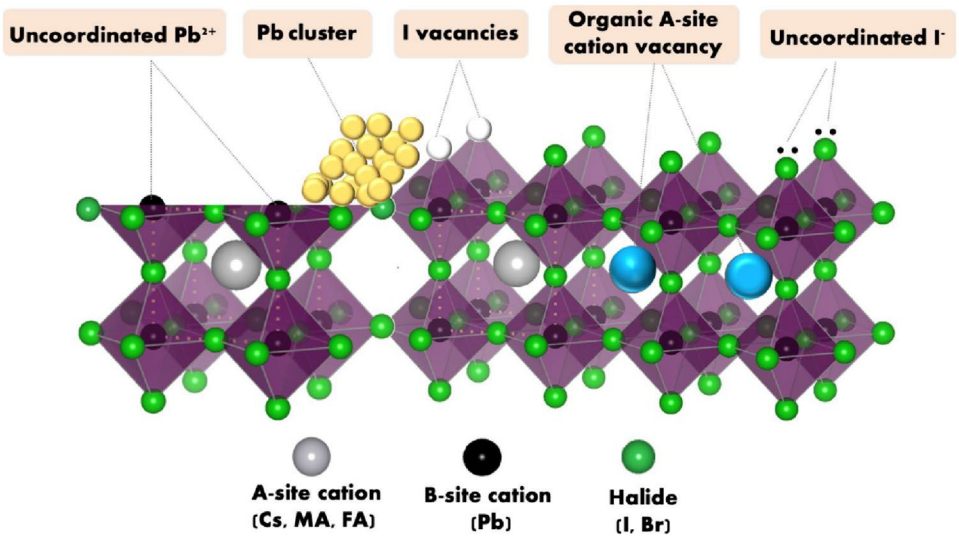

Fig. 15FF The possible surface defects of perovskite [146]

possess the mechanical robustness required for achieving compact structures in perovskite absorbers [147]. The quality of passivation in perovskite materials is influenced by the coordination of functional groups within the passivating material. The specific arrangement and bonding of these groups play a crucial role in determining the effectiveness of passivation. By optimizing the coordination chemistry, it is possible to enhance the passivation quality and improve the performance and stability of perovskite solar cells. Passivation by inorganic materials is becoming more popular due to this improved coordination. This section focuses on recent advancements in the performance of PSCs through the use of inorganic passivating materials. By optimizing the coordination chemistry, researchers aim to improve the overall performance and stability of PSCs. The most commonly utilized inorganic passivation materials for PSCs are classified as follows [148]:

1. Lead group containing materials, such as $PbSO_4$ and PbS, create comprehensive bandgap materials
2. Alkali metal halide materials, such as KPF_6, NaF, KI, and RbI, are primarily used for defect removal in interstitial ions
3. Transition metal halide materials, such as $NiCl_2$ and NbF_5, to passivate Pb-I anti-site defects
4. Halide based materials, such as CdI_2, GeI_2, ZnI_2, and $Cd(SCN_2H_4)_2Cl_2$, passivate vacancies, under coordinated anions.
5. Hydrophobic materials like thioctic acid (TA) form a protective layer against moisture and oxygen

Table 4 shows standard work recently reported by various researchers on inorganic additives. Chen et al. [149] introduced oleylamine (OA) derived $PbSO_4(PbO)_4$ quantum dots on HTL interface to passivate perovskites as well as improve the morphology of the films (see Table 4). The quantum dots have demonstrated multiple functions in enhancing the performance. These functions include passivating uncoordinated Pb^{2+} and I^- ions on the perovskite surface, forming robust hydrogen bonds with organic cations, and improving the chemical stability of the perovskite layer. The incorporation of quantum dots in PSCs has shown promising results in enhancing both the efficiency and stability of the devices. SEM imaging of the treated PSCs revealed improved surface morphology with fewer surface defects. Notably, the treated PSC device exhibited a higher PCE ranging from 20.02 to 16.86%, surpassing the performance of the untreated sample.

Yang et al. [150] used lead sulfate on the perovskite/HTL interface for physical protection (see Table 4). The introduction of a water insoluble lead (II) oxysalt effectively stabilized both the surface and bulk of the perovskite material by interacting with sulfate ions. This treatment improved the water tolerance of perovskite films by forming solid chemical connections and reducing defect density. As a result, the treated device demonstrated an extended charge carrier lifetime and enhanced solar cell efficiency, reaching 21.1%.

Wang et al. [151] performed interface modulation by potassium hexafluorophosphate (KPF_6) at different concentrations to promote charge carrier extraction and reduce charge recombination (see Table 4). A layer of KPF_6 was inserted between the SnO_2 quantum dot ETL and the perovskite layer. The KPF_6 reacted with the perovskite, causing reorientation and redistribution of the organic cation groups. It also reacted with the SnO_2 quantum dots, passivating interface defects and suppressing nonradiative recombination. PSCs treated with 0.5 mg/ml KPF_6 achieved a PCE of over 21%.

Bi et al. [152] employed KPF_6 to modify ETL/perovskite interface (see Table 4). Similar to previous research, KPF_6 improved the interfacial contact between the SnO_2

Table 4 Some data for improvements in PCE for inorganic additives for passivation of PSCs

Sr. no.	Name of additive (structure)	Perovskite + location	Type of additive	Passivation effect on	PCE (%) (% improvement)	References
1	Oleyl amine coated lead sulfate ($PbSO_4(PbO)_4$)	$MAPbI_3$ HTL interface	Inorganic non-halide (lead containing substance)	Uncoordinated Pb^{2+}	21.1 (12.83)	[149]
2	Lead sulfate ($PbSO_4$)	$Cs_{0.05}FA_{0.81}MA_{0.14}PbI_{2.55}Br_{0.45}$ perovskite/HTL interface	Inorganic non-halide (lead containing substance)	Uncoordinated Pb^{2+} and I^-	20.02 (18.74)	[150]
3	Potassium hexafluorophosphate (KPF_6)	$(CsI)_{0.04}(FAI)_{0.82}(PbI_2)_{0.86}(MAPbBr_3)_{0.14}$ between ETL and the perovskite layer	Inorganic halide (alkali metal halides)	SnO_2/perovskite interlayer	21 (23.23)	[151]
4	Potassium hexafluorophosphate (KPF_6)	$FA_{0.8}8Cs_{0.12}PbI_{3-x}(PF_6)_x$ ETL/perovskite interface	Inorganic halide (alkali metal halides)	SnO_2/perovskite interlayer	20.39 (3.72)	[152]
5	Nickel chloride ($NiCl_2$)	$MAPbI_3$ into perovskite precursor solution	Inorganic halide (transition metal halides)	δ-Phase	20.56 (12.35)	[153]
6	Cadmium iodide (CdI_2)	$MAPbI_3$ ETL/perovskite interface	Inorganic halide	Iodine vacancies	21.9 (8.41)	[154]
7	Thioctic acid (TA)	$MAPbI_3$ ETL interface	Organic non-halide (hydrophobic materials)	Pb-I anti-site defects	20.4 (17.24)	[155]
8	Lead sulfide (PbS_x)	$MAPbI_3$	Inorganic non-halide (lead containing substance)	Uncoordinated Pb^{2+}	18.54 (12.36)	[156]
9	Potassium iodide (KI)	$Cs_{0.06}FA_{0.79}MA_{0.15}Pb(I_{0.85}Br_{0.15})_3$	Inorganic halide (alkali metal halide)s	Iodide Frenkel defect	17.55 (2.39)	[157]
10	Rubidium iodide (RbI)	$MA_{0.5}FA_{0.5}PbI_3$	Inorganic halide (alkali metal halides)	Stability and hysteresis	21.8 (26.01)	[158]
11	Niobium fluoride (NbF_5)	$FA_{0.85}MA_{0.15}Pb_3$	Inorganic halide (transition metal halides)	δ-Phase	20.56 (12.34)	[159]
12	Zinc iodide (ZnI_2)	$CsPbI_2Br$	Inorganic halide	Grain boundary defects	12.16 (19.09)	[160]
13	Titanium oxide nanoparticles (TiO_2)	$MAPbI_3$	Inorganic non-halide (oxides)	Ion transports	17.42 (8.19)	[161, 162]
14	Zinc phthalocyanine (ZnPC)	$(ZnPc)_{0.5}MA_{n-1}PbnI_{3n+1}$	Inorganic non-halide (hydrophobic materials)	MA^+ migration	19.6 (4.25)	[163]

layer and the perovskite layer through hydrogen and coordination bonds. This modification resulted in a higher device efficiency of 21.39% from 19.66% of untreated device. The modified ETL layer showed improved surface quality without imperfections or pinholes.

Gong et al. [153] demonstrated that by dissolving $NiCl_2$ into a perovskite precursor solution, PbI^{3-} anti-site defects could be passivated (see Table 4). Due to the differing solubility of $NiCl_2$ and PbI_2, it was discovered that the addition of Ni^{2+} could considerably develop poly porous PbI_2 films, favoring MAI penetration and, therefore, forming bigger crystals. Here, the perovskite grain growth and defect passivation are accomplished simultaneously. As a result, a 3% Ni^{2+} addition-based PSC with improved cell stability may achieve a PCE of 20.6% under ambient conditions.

Wu et al. [154] modified the defects in the perovskite layer using cadmium iodide (CdI_2) between the ETL/perovskite interface (see Table 4). The addition of Cd-I interactions effectively stabilized iodine ions and reduced surface iodine shortage in the perovskite layer. This led to improved operating stability and reduced interfacial charge recombination loss. Blade-coated PSCs treated with Cd-I achieved a high power conversion efficiency (PCE) of 21.9%. The functional groups Cd^{2+}, I^-, and Cd-I played a crucial role in passivation. The thermal annealing process of the perovskite layer resulted in iodine vacancies on the surface, leading to nonradiative charge recombination and poor photocurrent. The Cd-I bond in the perovskite layer effectively stabilized iodide ions, compensating for the iodine deficiency and improving overall performance.

Chen et al. [155] demonstrated a cross-linkable small organic molecule thioctic acid (TA), anchored to ETL interface through complex bonds (see Table 4). Following thermal treatment, a robust continuous polymer (Poly(TA)) was formed in situ, acting as a bifacial passivation agent to reduce defects significantly. The addition of this layer has the potential to enhance charge extraction efficiency and improve the water and light resistance of the perovskite film. The carboxylic acid molecule (COOH) in the additive can coordinate with the surface of TiO_2, leading to improved performance. The presence of the 'S' type functional group in the TiO_2-Poly (TA) layer contributes to the formation of a high-quality perovskite film. As analyzed, contact angle increased dramatically from 30 to 102°, which aided in creating high-quality perovskite films. The poly (TA)-based device achieved a remarkable power conversion efficiency (PCE) of 20.4%, one of the highest reported for MAI-based perovskite, with minimal hysteresis.

Inorganic materials offer superior adhesion properties compared to organic materials, addressing the challenge of poor coupling between organic materials and perovskite layers. Strengthening the chemical connections with inorganic materials improves fault passivation, enhances stability, and provides mechanical protection, enhancing durability of PSCs. Inorganic materials are emerging as a potential strategy for passivation in perovskite solar cells (PSCs). Recent advancements demonstrate the diverse topologies and passivation effects of different inorganic materials. Some materials are effective within the perovskite layer, while others work at the interface. Combining these materials can yield promising results. Double-sided inorganic passivation, such as TA, offers intriguing research opportunities. Inorganic passivation materials with synergistic effects and the ability to passivate multiple faults and both sides can significantly enhance PSC performance and stability.

Summary and outlook

To achieve commercial viability, further advancements are needed to enhance the performance of perovskite solar cells (PSCs). While certain aspects like systematic engineering, structural design, charge transport, and electrode materials have made significant progress, additional research is required to improve stability and long-term operability. The enhancement in efficiency as well as stability is conceivable by addition of novel additive materials. It will lead to alter the surface morphology as well as crystalline structure. This review focuses on recent studies investigating the passivation of PSCs using neoteric energy materials, such as conducting polymer additives, MOFs, and other inorganic materials.

In conducting polymers, specific polymer structures with multiple required additive qualities must be formed by combining specific polarity gradations and then changing the polymer structures themselves. In reaction to environmental crises, technologies should be developed to use eco-friendly biodegradable polymers and environmentally sustainable materials above those that improve device performance. Essentially, conducting polymers considerably improve perovskite solar cell performance, leveraging their high conductivity for efficient charge transport and improving overall performance. The hydrophobicity of conducting polymers maintains high resistance to moisture, leading to superior stability. Actually, its low solubility, together with chemical modifications, augments material stability. Overcoming the challenging process-ability of conducting polymers involves utilizing self-assembly characteristics and scaffold structures. Polymer doping can further enhance conductivity, leading to improved superior efficiency. Essentially, due to its exclusive properties (both electrical as well as optical), conducting polymers enhance crystal morphology, crystal growth, and surface passivation. Serving as scaffolds for perovskite films, conducting polymers provide structural support, facilitating the formation of high-quality films. Encouraging reactions between PbI_2 and MAI is another contribution, promoting the development of stable perovskite structures. In summary, conducting polymers play a crucial role in improving key challenges of perovskite solar cells, including conductivity, hydrophobicity, solubility, and process-ability (see Table 1). Especially, PANI as additive imparts perovskite devices with better moisture and temperature resistance as discussed in detail.

Conversely, MOFs have distinct characteristics and are used in various locations throughout the PSC. MOFs are attractive for PSCs due to their tunable bandgaps, which can be easily adjusted by varying the components in straightforward synthesis processes. They exhibit varied physical and chemical characteristics that synergistically act on interstitial defects and thus they are a good choice for passivation additives in the future. By incorporating MOFs as additives, several researchers have demonstrated the ability to passivate defects, enhance charge transport, and improve the overall functionality of PSCs. MOFs can be used as additive at various locations in PSCs to enhance the quality of perovskite layer, charge transfer, and recombination mitigation. Additionally, they are interesting materials for PSCs as bandgaps can be simply tuned by altering the components. Besides, the porous structure of MOFs can act as protective barriers, improving stability by guarding perovskite layers from environmental factors. MOFs with scaffold structures facilitate controlled perovskite film growth, ensuring uniformity and enhanced device efficiency. The addition of MOFs therefore addresses vital

challenges in PSCs, favorable improvements in stability, efficiency, and overall performance. MOFs have an incredible potential to solve the device stability problem of PSCs.

Finally, inorganic compounds compensate for the inadequacies of organic additives by creating stronger bonds and playing a mechanical role in perovskite layer protection. To comprehensively impact PSC commercialization, various inorganic materials should be integrated and applied in device production methods.

In the current review article, different categories of materials used as an additive, namely, conducting polymers, MOFs, and inorganic additives are deliberated in depth. It is apparent that the maximum improvement (in both the PCE as well as stability) is relatively achieved by MOFs. Especially, zirconium-based MOFs led to superior improvement.

There is a great prospective for the commercial accomplishment of perovskite solar cells; if appropriate, additive materials are utilized appropriately during the fabrication of PSCs. Therefore, the existing review is to a great extent useful as a handy guide for further application of particular type of additive for the given perovskite.

In inference, the field of passivation studies holds immense potential for advancing photovoltaics. These types of passivating strategies can be useful for developing a PSC with a longer ambient operation lifetime leading to commercialization. So, further work on more such passivating strategies is required to be carried over in the near future. With the continuous development of new materials, there is a promising possibility for perovskite solar cells to rival traditional silicon solar cells, contributing to the resolution of energy challenges in the near future.

Acknowledgements The authors would like to thank Sardar Vallabhbhai National Institute of Technology, Surat, Government of India, and Department of Science and Technology, Government of India for help in carrying out the present work. We also acknowledge the sophisticated Instrument Centre, SVNIT, Surat for characterization facilities.

Author contribution Srish Kulkarni: literature survey, classification, investigation, and writing original draft. Dr. Smita Gupta: writing review and editing. Dr. Jignasa V. Gohel: conceptualization, experimental design, supervision, writing review and editing, validation, project administration, and funding acquisition.

Data and code availability Not applicable.

Declarations

Ethical approval No experiments involving human tissue were carried out, so no ethical approval was required by an institutional review board or equivalent ethics committee.

Competing interests The authors declare no competing interests.

References

1. Jeong J, Kim M, Seo J, Lu H, Ahlawat P, Mishra A, Yang Y, Hope MA, Eickemeyer FT, Kim M, Yoon YJ, Choi IW, Darwich BP, Choi SJ, Jo Y, Lee JH, Walker B, Zakeeruddin SM, Emsley L, Rothlisberger U, Hagfeldt A, Kim DS, Grätzel M, Kim JY (2021) Pseudo-halide anion engineering for α-FAPbI3 perovskite solar cells. Nature 592(7854):381–385. https://doi.org/10.1038/s41586-021-03406-5
2. Yang WS, Noh JH, Jeon NJ, Kim YC, Ryu S, Seo J, Seok S Il (2015) High-performance photovoltaic perovskite layers fabricated through intramolecular exchange. Science (1979) 348(6240):1234–1237. https://doi.org/10.1126/science.aaa9272
3. Burschka J, Pellet N, Moon S-J, Humphry-Baker R, Gao P, Nazeeruddin MK, Grätzel M (2013) Sequential deposition as a route to high-performance perovskite-sensitized solar cells. Nature 499(7458):316–319. https://doi.org/10.1038/nature12340
4. Chen W, Wu Y, Yue Y, Liu J, Zhang W, Yang X, Chen H, Bi E, Ashraful I, Grätzel M, Han L (2015) Efficient and stable large-area perovskite solar cells with inorganic charge extraction layers. Science (1979) 350(6263):944–948. https://doi.org/10.1126/science.aad1015
5. Yin W-J, Shi T, Yan Y (2014) Unique properties of halide perovskites as possible origins of the superior solar cell performance. Adv Mater 26(27):4653–4658. https://doi.org/10.1002/adma.201306281
6. Cheng X, Yang S, Cao B, Tao X, Chen Z (2020) Single crystal perovskite solar cells: development and perspectives. Adv Funct Mater Wiley-VCH Verlag. https://doi.org/10.1002/adfm.201905021
7. Huang J, Yuan Y, Shao Y, Yan Y (2017) Understanding the physical properties of hybrid perovskites for photovoltaic applications. Nat Rev Mater 2(7):17042. https://doi.org/10.1038/natrevmats.2017.42
8. Huang J, Shao Y, Dong Q (2015) Organometal trihalide perovskite single crystals: a next wave of materials for 25% efficiency photovoltaics and applications beyond? J Phys Chem Lett 6(16):3218–3227. https://doi.org/10.1021/acs.jpclett.5b01419
9. Saki Z, Byranvand MM, Taghavinia N, Kedia M, Saliba M (2021) Solution-processed perovskite thin-films: the journey from lab- to large-scale solar cells. Energy Environ Sci 14(11):5690–5722. https://doi.org/10.1039/D1EE02018H
10. Razza S, Castro-Hermosa S, Di Carlo A, Brown TM (2016) Research update: large-area deposition, coating, printing, and processing techniques for the upscaling of perovskite solar cell technology. APL Mater 4(9):091508. https://doi.org/10.1063/1.4962478
11. Cai M, Wu Y, Chen H, Yang X, Qiang Y, Han L (2017) Cost-performance analysis of perovskite solar modules. Adv Sci 4(1):1600269. https://doi.org/10.1002/advs.201600269
12. Li Z, Zhao Y, Wang X, Sun Y, Zhao Z, Li Y, Zhou H, Chen Q (2018) Cost analysis of perovskite tandem photovoltaics. Joule 2(8):1559–1572. https://doi.org/10.1016/j.joule.2018.05.001
13. Niu G, Guo X, Wang L (2015) Review of recent progress in chemical stability of perovskite solar cells. J Mater Chem A Mater 3(17):8970–8980. https://doi.org/10.1039/c4ta04994b
14. Agiorgousis ML, Sun Y-Y, Zeng H, Zhang S (2014) Strong covalency-induced recombination centers in perovskite solar cell material $CH_3NH_3PbI_3$. J Am Chem Soc 136(41):14570–14575. https://doi.org/10.1021/ja5079305
15. Yin W-J, Shi T, Yan Y (2014) Unusual defect physics in $CH_3NH_3PbI_3$ perovskite solar cell absorber. Appl Phys Lett 104(6):063903. https://doi.org/10.1063/1.4864778

16. Steirer KX, Schulz P, Teeter G, Stevanovic V, Yang M, Zhu K, Berry JJ (2016) Defect tolerance in methylammonium lead triiodide perovskite. ACS Energy Lett 1(2):360–366. https://doi.org/10.1021/acsenergylett.6b00196
17. Walsh A, Scanlon DO, Chen S, Gong XG, Wei S (2015) Self-regulation mechanism for charged point defects in hybrid halide perovskites. Angew Chem Int Ed 54(6):1791–1794. https://doi.org/10.1002/anie.201409740
18. Kim J, Lee S-H, Lee JH, Hong K-H (2014) The role of intrinsic defects in methylammonium lead iodide perovskite. J Phys Chem Lett 5(8):1312–1317. https://doi.org/10.1021/jz500370k
19. Ball JM, Petrozza A (2016) Defects in perovskite-halides and their effects in solar cells. Nat Energy 1(11):16149. https://doi.org/10.1038/nenergy.2016.149
20. Stranks SD (2017) Nonradiative losses in metal halide perovskites. ACS Energy Lett 2(7):1515–1525. https://doi.org/10.1021/acsenergylett.7b00239
21. Li N, Niu X, Chen Q, Zhou H (2020) Towards commercialization: the operational stability of perovskite solar cells. Chem Soc Rev 49(22):8235–8286. https://doi.org/10.1039/d0cs00573h
22. Mahapatra A, Prochowicz D, Tavakoli MM, Trivedi S, Kumar P, Yadav P (2020) A review of aspects of additive engineering in perovskite solar cells. J Mater Chem A Mater 8(1):27–54. https://doi.org/10.1039/C9TA07657C
23. Jiang Q, Zhao Y, Zhang X, Yang X, Chen Y, Chu Z, Ye Q, Li X, Yin Z, You J (2019) Surface passivation of perovskite film for efficient solar cells. Nat Photonics 13(7):460–466. https://doi.org/10.1038/s41566-019-0398-2
24. Patel SB, Gohel JV (2018) Optimization of sol–gel spin-coated Cu2ZnSnS4 (CZTS) thin-film control parameters by RSM method to enhance the solar cell performance. J Mater Sci 53:12203–12213. https://doi.org/10.1007/s10853-018-2464-4
25. Patel SB, Gohel JV (2018) Synthesis of novel counter electrode by combination of mesoporous–macroporous CZTS films for enhanced performance of quantum-dots sensitized solar cells. J Mater Sci Mater Electron 29(21):18151–18158
26. Kumari N, Patel SR, Gohel JV (2020) Optimization of MAPbI3 film using response surface methodology for enhancement in photovoltaic performance. In: L Ledwani, JS Sangwai (eds.) Nanotechnology for Energy and Environmental Engineering- Part of the Green Energy and Technology book series. Springer International Publishing, pp 395-412.
27. Nair S, Gohel JV (2021) Impact of stress testing and passivation strategies on low-cost carbon-based perovskite solar cell under ambient conditions. Opt Mater 117:111214. https://doi.org/10.1016/j.optmat.2021.111214
28. Nair S, Gohel JV (2021) Introduction of P3HT-based gradient heterojunction layer to improve optoelectronic performance of low-cost carbon-based perovskite solar cell. Opt Mater 119:111366. https://doi.org/10.1016/j.optmat.2021.111366
29. Khare S, Gohel JV (2022) Performance enhancement of cost-effective mixed cationic perovskite solar cell with MgCl2 and n-BAI as surface passivating agents. Opt Mater 132:112845. https://doi.org/10.1016/j.optmat.2022.112845
30. Kulkarni S, Gupta S, Gohel JV (2023) Incorporation of MOF UiO-66-NH2 and polyaniline for enhanced performance of low-cost carbon-based perovskite solar cells. Opt Mater 144:114268. https://doi.org/10.1016/j.optmat.2023.114268
31. Zhang Z, Qiao L, Meng K, Long R, Chen G, Gao P (2023) Rationalization of passivation strategies toward high-performance perovskite solar cells. Chem Soc Rev 52(1):163–195. https://doi.org/10.1039/D2CS00217E
32. Mohd Yusoff bin Adb R, Vasilopoulou M, Georgiadou DG, Palilis LC, Abate A, Nazeeruddin MK (2021) Passivation and process engineering approaches of halide perovskite films for high efficiency and stability perovskite solar cells. Energy Environ Sci 14(5):2906–2953. https://doi.org/10.1039/D1EE00062D
33. Yang R, Ji Y, Li Q, Zhao Z, Zhang R, Liang L, Liu F, Chen Y, Han S, Yu X, Liu H (2019) Ultrafine Si nanowires/Sn3O4 nanosheets 3D hierarchical heterostructured array as a photoanode with high-efficient photoelectrocatalytic performance. Appl Catal B 256:117798. https://doi.org/10.1016/j.apcatb.2019.117798
34. Zhao J, Liu F, Wang W, Wang Y, Wen N, Zhang Z, Dai W, Yuan R, Ding Z, Long J (2023) S-scheme-heterojunction $LaNiO_3$ /$CdLa_2S_4$ photocatalyst for solar-driven CO_2 -to-CO conversion. ACS Appl Nano Mater 6(10):8927–8936. https://doi.org/10.1021/acsanm.3c01443
35. Zhao J, Huang Q, Xie Z, Liu Y, Liu F, Wei F, Wang S, Zhang Z, Yuan R, Wu K, Ding Z, Long J (2023) Hierarchical hollow-TiO_2 @CdS/ZnS hybrid for solar-driven CO_2 -selective conversion. ACS Appl Mater Interfaces 15(20):24494–24503. https://doi.org/10.1021/acsami.3c03255
36. Zhao J, Huang L, Xue L, Niu Z, Zhang Z, Ding Z, Yuan R, Lu X, Long J (2023) Selectively converting CO2 to HCOOH on Cu-alloys integrated in hematite-driven artificial photosynthetic cells. J Energy Chem 79:601–610. https://doi.org/10.1016/j.jechem.2022.12.062
37. Zhao J, Xue L, Niu Z, Huang L, Hou Y, Zhang Z, Yuan R, Ding Z, Fu X, Lu X, Long J (2021) Conversion of CO2 to formic acid by integrated all-solar-driven artificial photosynthetic system. J Power Sources 512:230532. https://doi.org/10.1016/j.jpowsour.2021.230532
38. Das TK, Prusty S (2012) Review on conducting polymers and their applications. Polym Plast Technol Eng 51(14):1487–1500. https://doi.org/10.1080/03602559.2012.710697
39. Umoren SA, Solomon MM, Saji VS (2022) Conducting polymers. In: Polymeric materials in corrosion inhibition. Elsevier, pp 443–466. https://doi.org/10.1016/B978-0-12-823854-7.00002-3
40. Nalwa H (2000) Index for volume 5. In: Handbook of Nanostructured Materials and Nanotechnology. Elsevier, pp 769–778. https://doi.org/10.1016/B978-012513760-7/50070-8
41. Naarmann H (2000) Polymers, electrically conducting. In: Ullmann's encyclopedia of industrial chemistry. Wiley-VCH Verlag GmbH & Co, Weinheim, Germany. https://doi.org/10.1002/14356007.a21_429
42. K, N., Rout, C. S. (2021) Conducting polymers: a comprehensive review on recent advances in synthesis, properties and applications. RSC Adv 11(10):5659–5697. https://doi.org/10.1039/D0RA07800J
43. Han T-H, Lee J-W, Choi C, Tan S, Lee C, Zhao Y, Dai Z, De Marco N, Lee S-J, Bae S-H, Yuan Y, Lee HM, Huang Y, Yang Y (2019) Perovskite-polymer composite cross-linker approach for highly-stable and efficient perovskite solar cells. Nat Commun 10(1):520. https://doi.org/10.1038/s41467-019-08455-z
44. Brédas J-L, Beljonne D, Coropceanu V, Cornil J (2004) Charge-transfer and energy-transfer processes in π-conjugated oligomers and polymers: a molecular picture. Chem Rev 104(11):4971–5004. https://doi.org/10.1021/cr040084k
45. Yan W, Li Y, Li Y, Ye S, Liu Z, Wang S, Bian Z, Huang C (2015) High-performance hybrid perovskite solar cells with open circuit voltage dependence on hole-transporting materials. Nano Energy 16:428–437. https://doi.org/10.1016/j.nanoen.2015.07.024
46. Darmanin T, Guittard F (2014) Wettability of conducting polymers: from superhydrophilicity to superoleophobicity. Prog Polym Sci 39(4):656–682. https://doi.org/10.1016/j.progpolymsci.2013.10.003
47. Eperon GE, Stranks SD, Menelaou C, Johnston MB, Herz LM, Snaith HJ (2014) Formamidinium lead trihalide: a broadly tunable perovskite for efficient planar heterojunction solar cells. Energy Environ Sci 7(3):982. https://doi.org/10.1039/c3ee43822h

48. Jeon NJ, Noh JH, Kim YC, Yang WS, Ryu S, Seok S Il (2014) Solvent engineering for high-performance inorganic–organic hybrid perovskite solar cells. Nat Mater 13(9):897–903. https://doi.org/10.1038/nmat4014
49. Tidhar Y, Edri E, Weissman H, Zohar D, Hodes G, Cahen D, Rybtchinski B, Kirmayer S (2014) Crystallization of methyl ammonium lead halide perovskites: implications for photovoltaic applications. J Am Chem Soc 136(38):13249–13256. https://doi.org/10.1021/ja505556s
50. Bi D, Yi C, Luo J, Décoppet J-D, Zhang F, Zakeeruddin SM, Li X, Hagfeldt A, Grätzel M (2016) Polymer-templated nucleation and crystal growth of perovskite films for solar cells with efficiency greater than 21%. Nat Energy 1(10):16142. https://doi.org/10.1038/nenergy.2016.142
51. Peng J, Khan JI, Liu W, Ugur E, Duong T, Wu Y, Shen H, Wang K, Dang H, Aydin E, Yang X, Wan Y, Weber KJ, Catchpole KR, Laquai F, Wolf S, White TP (2018) A universal double-side passivation for high open-circuit voltage in perovskite solar cells: role of carbonyl groups in poly(methyl methacrylate). Adv Energy Mater 8(30):1801208. https://doi.org/10.1002/aenm.201801208
52. Bischak CG, Sanehira EM, Precht JT, Luther JM, Ginsberg NS (2015) Heterogeneous charge carrier dynamics in organic–inorganic hybrid materials: nanoscale lateral and depth-dependent variation of recombination rates in methylammonium lead halide perovskite thin films. Nano Lett 15(7):4799–4807. https://doi.org/10.1021/acs.nanolett.5b01917
53. Lee J-W, Bae S-H, Hsieh Y-T, De Marco N, Wang M, Sun P, Yang Y (2017) A bifunctional lewis base additive for microscopic homogeneity in perovskite solar cells. Chem 3(2):290–302. https://doi.org/10.1016/j.chempr.2017.05.020
54. Brenes R, Guo D, Osherov A, Noel NK, Eames C, Hutter EM, Pathak SK, Niroui F, Friend RH, Islam MS, Snaith HJ, Bulović V, Savenije TJ, Stranks SD (2017) Metal halide perovskite polycrystalline films exhibiting properties of single crystals. Joule 1(1):155–167. https://doi.org/10.1016/j.joule.2017.08.006
55. Kim K, Han J, Maruyama S, Balaban M, Jeon I (2021) Role and contribution of polymeric additives in perovskite solar cells: crystal growth templates and grain boundary passivators. Solar RRL 5(5):2000783. https://doi.org/10.1002/solr.202000783
56. Firda PBD, Malik YT, Oh JK, Wujcik EK, Jeon J-W (2021) Enhanced chemical and electrochemical stability of polyaniline-based layer-by-layer films. Polymers (Basel) 13(17):2992. https://doi.org/10.3390/polym13172992
57. Araujo JR, Lopes ES, de Castro RK, Senna CA, de Robertis E, Neves RS, Fragneaud B, Nykänen A, Kuznetsov A, Archanjo BS, De Paoli MA (2018) Chapter 8 - characterization of polyaniline-based blends, composites, and nanocomposites, editor(s): P.M. Visakh, Cristina Della Pina, Ermelinda Falletta, Polyaniline Blends, Composites, and Nanocomposites, Elsevier, 209–233, ISBN 9780128095515. https://doi.org/10.1016/B978-0-12-809551-5.00008-4
58. Beygisangchin M, Abdul Rashid S, Shafie S, Sadrolhosseini AR, Lim HN (2021) Preparations, properties, and applications of polyaniline and polyaniline thin films—a review. Polymers (Basel) 13(12):2003. https://doi.org/10.3390/polym13122003
59. Kim DI, Lee JW, Jeong RH, Boo J-H (2022) A high-efficiency and stable perovskite solar cell fabricated in ambient air using a polyaniline passivation layer. Sci Rep 12(1):697. https://doi.org/10.1038/s41598-021-04547-3
60. Naji AM, Kareem SH, Faris AH, Mohammed MKA (2021) Polyaniline polymer-modified ZnO electron transport material for high-performance planar perovskite solar cells. Ceram Int 47(23):33390–33397. https://doi.org/10.1016/j.ceramint.2021.08.244
61. Zheng H, Xu X, Xu S, Liu G, Chen S, Zhang X, Chen T, Pan X (2019) The multiple effects of polyaniline additive to improve the efficiency and stability of perovskite solar cells. J Mater Chem C Mater 7(15):4441–4448. https://doi.org/10.1039/C8TC05975F
62. Mei Y, Shen Z, Kundu S, Dennis E, Pang S, Tan F, Yue G, Gao Y, Dong C, Liu R, Zhang W, Saidaminov MI (2021) Perovskite solar cells with polyaniline hole transport layers surpassing a 20% power conversion efficiency. Chem Mater 33(12):4679–4687. https://doi.org/10.1021/acs.chemmater.1c01176
63. Abdelmagid A, El Tahan A, Habib M, Anas M, Soliman M (2020) Effect of different ratios of polyaniline:poly(styrene sulfonate) on the hole extraction ability in perovskite solar cells. Synth Met 259:116232. https://doi.org/10.1016/j.synthmet.2019.116232
64. Lee K, Yu H, Lee JW, Oh J, Bae S, Kim SK, Jang J (2018) Efficient and moisture-resistant hole transport layer for inverted perovskite solar cells using solution-processed polyaniline. J Mater Chem C Mater 6(23):6250–6256. https://doi.org/10.1039/C8TC01870G
65. Lim K-G, Ahn S, Kim H, Choi M-R, Huh DH, Lee T-W (2016) Self-doped conducting polymer as a hole-extraction layer in organic-inorganic hybrid perovskite solar cells. Adv Mater Interfaces 3(9):1500678. https://doi.org/10.1002/admi.201500678
66. Chen J-Y, Yu M-H, Chang S-F, Wen Sun K (2013) Highly efficient poly(3,4-ethylenedioxythiophene):poly(styrenesulfonate)/Si hybrid solar cells with imprinted nanopyramid structures. Appl Phys Lett 103(13):133901. https://doi.org/10.1063/1.4822116
67. Lakdusinghe M, Abbaszadeh M, Mishra S, Sengottuvelu D, Wijayapala R, Zhang S, Benasco AR, Gu X, Morgan SE, Wipf DO, Kundu S (2021) Nanoscale self-assembly of poly(3-hexylthiophene) assisted by a low-molecular-weight gelator toward large-scale fabrication of electrically conductive networks. ACS Appl Nano Mater 4(8):8003–8014. https://doi.org/10.1021/acsanm.1c01294
68. Zhang S, Yan H, Yeh J, Shi X, Zhang P (2019) Electroactive composite of $FeCl_3$-doped P3HT/PLGA with adjustable electrical conductivity for potential application in neural tissue engineering. Macromol Biosci 19(10):1900147. https://doi.org/10.1002/mabi.201900147
69. Tang K, Huang L, Lim J, Zaveri T, Azoulay JD, Guo S (2019) Chemical doping of well-dispersed P3HT thin-film nanowire networks. ACS Appl Polym Mater 1(11):2943–2950. https://doi.org/10.1021/acsapm.9b00653
70. Sharma T, Singhal R, Vishnoi R, Lakshmi GBVS, Chand S, Avasthi DK, Kanjilal A, Biswas SK (2017) Ion irradiation induced modifications of P3HT: a donor material for organic photovoltaic devices. Vacuum 135:73–85. https://doi.org/10.1016/j.vacuum.2016.10.027
71. Hai TAP, Sugimoto R (2018) Surface functionalization of cellulose with poly(3-hexylthiophene) via novel oxidative polymerization. Carbohydr Polym 179:221–227. https://doi.org/10.1016/j.carbpol.2017.09.067
72. Mehmood U, Al-Ahmed A, Hussein IA (2016) Review on recent advances in polythiophene based photovoltaic devices. Renew Sustain Energy Rev 57:550–561. https://doi.org/10.1016/j.rser.2015.12.177
73. McQuade DT, Pullen AE, Swager TM (2000) Conjugated polymer-based chemical sensors. Chem Rev 100(7):2537–2574. https://doi.org/10.1021/cr9801014
74. Nielsen CB, McCulloch I (2013) Recent advances in transistor performance of polythiophenes. Prog Polym Sci 38(12):2053–2069. https://doi.org/10.1016/j.progpolymsci.2013.05.003
75. Xie H, Liu J, Yin X, Guo Y, Liu D, Wang G, Que W (2022) Perovskite/P3HT graded heterojunction by an additive-assisted method for high-efficiency perovskite solar cells with carbon electrodes. Colloids Surf A Physicochem Eng Asp 635:128072. https://doi.org/10.1016/j.colsurfa.2021.128072

76. Nair S, Gohel JV (2021) Introduction of P3HT-based gradient heterojunction layer to improve optoelectronic performance of low-cost carbon-based perovskite solar cell. Opt Mater (Amst) 119:111366. https://doi.org/10.1016/j.optmat.2021.111366
77. Dicker G, de Haas MP, Siebbeles LDA, Warman JM (2004) Electrodeless time-resolved microwave conductivity study of charge-carrier photogeneration in regioregular poly(3-hexylthiophene) thin films. Phys Rev B 70(4):045203. https://doi.org/10.1103/PhysRevB.70.045203
78. Jiang M, Yuan J, Cao G, Tian J (2020) In-situ fabrication of P3HT passivating layer with hole extraction ability for enhanced performance of perovskite solar cell. Chem Eng J 402:126152. https://doi.org/10.1016/j.cej.2020.126152
79. Wang G, Dong W, Gurung A, Chen K, Wu F, He Q, Pathak R, Qiao Q (2019) Improving photovoltaic performance of carbon-based CsPbBr 3 perovskite solar cells by interfacial engineering using P3HT interlayer. J Power Sources 432:48–54. https://doi.org/10.1016/j.jpowsour.2019.05.075
80. Groenendaal L, Jonas F, Freitag D, Pielartzik H, Reynolds JR (2000) Poly(3,4-ethylenedioxythiophene) and its derivatives: past, present, and future. Adv Mater 12(7):481–494. https://doi.org/10.1002/(SICI)1521-4095(200004)12:7%3c481::AID-ADMA481%3e3.0.CO;2-C
81. Root SE, Savagatrup S, Printz AD, Rodriquez D, Lipomi DJ (2017) Mechanical properties of organic semiconductors for stretchable, highly flexible, and mechanically robust electronics. Chem Rev 117(9):6467–6499. https://doi.org/10.1021/acs.chemrev.7b00003
82. Ha SR, Park S, Oh JT, Kim DH, Cho S, Bae SY, Kang D-W, Kim J-M, Choi H (2018) Water-resistant PEDOT:PSS hole transport layers by incorporating a photo-crosslinking agent for high-performance perovskite and polymer solar cells. Nanoscale 10(27):13187–13193. https://doi.org/10.1039/C8NR02903B
83. Qi Y, Almtiri M, Giri H, Jha S, Ma G, Shaik AK, Zhang Q, Pradhan N, Gu X, Hammer NI, Patton D, Scott C, Dai Q (2022) Evaluation of the passivation effects of PEDOT:PSS on inverted perovskite solar cells. Adv Energy Mater 12(46):2202713. https://doi.org/10.1002/aenm.202202713
84. Karbovnyk I, Olenych I, Aksimentyeva O, Klym H, Dzendzelyuk O, Olenych Y, Hrushetska O (2016) Effect of radiation on the electrical properties of PEDOT-based nanocomposites. Nanoscale Res Lett 11(1):84. https://doi.org/10.1186/s11671-016-1293-0
85. Wu F, Yan K, Wu H, Niu B, Liu Z, Li Y, Zuo L, Chen H (2021) Tuning interfacial chemical interaction for high-performance perovskite solar cell with PEDOT:PSS as hole transporting layer. J Mater Chem A Mater 9(26):14920–14927. https://doi.org/10.1039/D1TA03024H
86. Wang M, Wang H, Li W, Hu X, Sun K, Zang Z (2019) Defect passivation using ultrathin PTAA layers for efficient and stable perovskite solar cells with a high fill factor and eliminated hysteresis. J Mater Chem A Mater 7(46):26421–26428. https://doi.org/10.1039/C9TA08314F
87. Zhou X, Hu M, Liu C, Zhang L, Zhong X, Li X, Tian Y, Cheng C, Xu B (2019) Synergistic effects of multiple functional ionic liquid-treated PEDOT:PSS and less-ion-defects S-acetylthiocholine chloride-passivated perovskite surface enabling stable and hysteresis-free inverted perovskite solar cells with conversion efficiency over 20%. Nano Energy 63:103866. https://doi.org/10.1016/j.nanoen.2019.103866
88. Jiao L, Seow JYR, Skinner WS, Wang ZU, Jiang H-L (2019) Metal–organic frameworks: structures and functional applications. Mater Today 27:43–68. https://doi.org/10.1016/j.mattod.2018.10.038
89. Meng W, Kondo S, Ito T, Komatsu K, Pirillo J, Hijikata Y, Ikuhara Y, Aida T, Sato H (2021) An elastic metal–organic crystal with a densely catenated backbone. Nature 598(7880):298–303. https://doi.org/10.1038/s41586-021-03880-x
90. Dias EM, Petit C (2015) Towards the use of metal–organic frameworks for water reuse: a review of the recent advances in the field of organic pollutants removal and degradation and the next steps in the field. J Mater Chem A Mater 3(45):22484–22506. https://doi.org/10.1039/C5TA05440K
91. Li H, Wang K, Sun Y, Lollar CT, Li J, Zhou H-C (2018) Recent advances in gas storage and separation using metal–organic frameworks. Mater Today 21(2):108–121. https://doi.org/10.1016/j.mattod.2017.07.006
92. Hu YH, Zhang L (2010) Hydrogen storage in metal-organic frameworks. Adv Mater 22(20):E117–E130. https://doi.org/10.1002/adma.200902096
93. Wu S, Li Z, Li M-Q, Diao Y, Lin F, Liu T, Zhang J, Tieu P, Gao W, Qi F, Pan X, Xu Z, Zhu Z, Jen AK-Y (2020) 2D metal–organic framework for stable perovskite solar cells with minimized lead leakage. Nat Nanotechnol 15(11):934–940. https://doi.org/10.1038/s41565-020-0765-7
94. Silva CG, Corma A, García H (2010) Metal–organic frameworks as semiconductors. J Mater Chem 20(16):3141. https://doi.org/10.1039/b924937k
95. Cheng W, Zhang H, Luan D, Lou XW (David) (2021) Exposing unsaturated Cu $_1$ -O $_2$ sites in nanoscale Cu-MOF for efficient electrocatalytic hydrogen evolution. Sci Adv 7(18):eabg2580. https://doi.org/10.1126/sciadv.abg2580
96. Wang H, Zou H, Liu Y, Liu Z, Sun W, Lin KA, Li T, Luo S (2021) Ni2P nanocrystals embedded Ni-MOF nanosheets supported on nickel foam as bifunctional electrocatalyst for urea electrolysis. Sci Rep 11(1):21414. https://doi.org/10.1038/s41598-021-00776-8
97. Sharma A, Lim J, Jeong S, Won S, Seong J, Lee S, Kim YS, Baek SB, Lah MS (2021) Superprotonic conductivity of MOF-808 achieved by controlling the binding mode of grafted sulfamate. Angew Chem Int Ed 60(26):14334–14338. https://doi.org/10.1002/anie.202103191
98. Heo DY, Do HH, Ahn SH, Kim SY (2020) Metal-organic framework materials for perovskite solar cells. Polymers (Basel) 12(9):2061. https://doi.org/10.3390/polym12092061
99. Rosi NL, Eckert J, Eddaoudi M, Vodak DT, Kim J, O'Keeffe M, Yaghi OM (2003) Hydrogen storage in microporous metal-organic frameworks. Science (1979) 300(5622):1127–1129. https://doi.org/10.1126/science.1083440
100. Surblé S, Serre C, Mellot-Draznieks C, Millange F, Férey G (2006) A new isoreticular class of metal-organic-frameworks with the MIL-88 topology. Chem Commun 3:284–286. https://doi.org/10.1039/B512169H
101. Ma S, Sun D, Simmons JM, Collier CD, Yuan D, Zhou H-C (2008) Metal-organic framework from an anthracene derivative containing nanoscopic cages exhibiting high methane uptake. J Am Chem Soc 130(3):1012–1016. https://doi.org/10.1021/ja0771639
102. Wang B, Côté AP, Furukawa H, O'Keeffe M, Yaghi OM (2008) Colossal cages in zeolitic imidazolate frameworks as selective carbon dioxide reservoirs. Nature 453(7192):207–211. https://doi.org/10.1038/nature06900
103. Cavka JH, Jakobsen S, Olsbye U, Guillou N, Lamberti C, Bordiga S, Lillerud KP (2008) A new zirconium inorganic building brick forming metal organic frameworks with exceptional stability. J Am Chem Soc 130(42):13850–13851. https://doi.org/10.1021/ja8057953
104. Yang Q, Wiersum AD, Llewellyn PL, Guillerm V, Serre C, Maurin G (2011) Functionalizing porous zirconium terephthalate UiO-66(Zr) for natural gas upgrading: a computational exploration. Chem Commun 47(34):9603. https://doi.org/10.1039/c1cc13543k

105. Shen M, Zhang Y, Xu H, Ma H (2021) MOFs based on the application and challenges of perovskite solar cells. iScience 24(9):103069. https://doi.org/10.1016/j.isci.2021.103069
106. Lu H, Zhong J, Ji C, Zhao J, Li D, Zhao R, Jiang Y, Fang S, Liang T, Li H, Li CM (2020) Fabricating an optimal rutile TiO_2 electron transport layer by delicately tuning TiCl4 precursor solution for high performance perovskite solar cells. Nano Energy 68:104336. https://doi.org/10.1016/j.nanoen.2019.104336
107. Seo J-Y, Kim H-S, Akin S, Stojanovic M, Simon E, Fleischer M, Hagfeldt A, Zakeeruddin SM, Grätzel M (2018) Novel P-dopant toward highly efficient and stable perovskite solar cells. Energy Environ Sci 11(10):2985–2992. https://doi.org/10.1039/C8EE01500G
108. Zhai S, Karahan HE, Wang C, Pei Z, Wei L, Chen Y (2020) 1D supercapacitors for emerging electronics: current status and future directions. Adv Mater 32(5):1902387. https://doi.org/10.1002/adma.201902387
109. Liu Y, Hu Y, Zhang X, Zeng P, Li F, Wang B, Yang Q, Liu M (2020) Inhibited aggregation of lithium salt in spiro-OMeTAD toward highly efficient perovskite solar cells. Nano Energy 70:104483. https://doi.org/10.1016/j.nanoen.2020.104483
110. Chueh C-C, Chen C-I, Su Y-A, Konnerth H, Gu Y-J, Kung C-W, Wu KC-W (2019) Harnessing MOF materials in photovoltaic devices: recent advances, challenges, and perspectives. J Mater Chem A Mater 7(29):17079–17095. https://doi.org/10.1039/C9TA03595H
111. Ahmadian-Yazdi M-R, Gholampour N, Eslamian M (2020) Interface engineering by employing zeolitic imidazolate framework-8 (ZIF-8) as the only scaffold in the architecture of perovskite solar cells. ACS Appl Energy Mater 3(4):3134–3143. https://doi.org/10.1021/acsaem.9b02115
112. Sadegh F, Akin S, Moghadam M, Mirkhani V, Ruiz-Preciado MA, Wang Z, Tavakoli MM, Graetzel M, Hagfeldt A, Tress W (2020) Highly efficient, stable and hysteresis-less planar perovskite solar cell based on chemical bath treated Zn2SnO4 electron transport layer. Nano Energy 75:105038. https://doi.org/10.1016/j.nanoen.2020.105038
113. Nguyen TMH, Bark CW (2020) Synthesis of cobalt-doped TiO_2 based on metal–organic frameworks as an effective electron transport material in perovskite solar cells. ACS Omega 5(5):2280–2286. https://doi.org/10.1021/acsomega.9b03507
114. Ji J, Liu B, Huang H, Wang X, Yan L, Qu S, Liu X, Jiang H, Duan M, Li Y, Li M (2021) Nondestructive passivation of the TiO_2 electron transport layer in perovskite solar cells by the PEIE-2D MOF interfacial modified layer. J Mater Chem C Mater 9(22):7057–7064. https://doi.org/10.1039/D1TC00036E
115. Liu S, Huang W, Liao P, Pootrakulchote N, Li H, Lu J, Li J, Huang F, Shai X, Zhao X, Shen Y, Cheng Y-B, Wang M (2017) 17% efficient printable mesoscopic PIN metal oxide framework perovskite solar cells using cesium-containing triple cation perovskite. J Mater Chem A Mater 5(44):22952–22958. https://doi.org/10.1039/C7TA07660F
116. Wang J, Zhang J, Yang Y, Dong Y, Wang W, Hu B, Li J, Cao W, Lin K, Xia D, Fan R (2022) Li-TFSI endohedral metal-organic frameworks in stable perovskite solar cells for anti-deliquescent and restricting ion migration. Chem Eng J 429:132481. https://doi.org/10.1016/j.cej.2021.132481
117. Zhang J, Guo S, Zhu M, Li C, Chen J, Liu L, Xiang S, Zhang Z (2021) Simultaneous defect passivation and hole mobility enhancement of perovskite solar cells by incorporating anionic metal-organic framework into hole transport materials. Chem Eng J 408:127328. https://doi.org/10.1016/j.cej.2020.127328
118. Geng C, Xie Y, Wei P, Liu H, Qiang Y, Zhang Y (2020) An efficient Co-NC composite additive for enhancing interface performance of carbon-based perovskite solar cells. Electrochim Acta 358:136883. https://doi.org/10.1016/j.electacta.2020.136883
119. Hazeghi F, Mozaffari S, Ghorashi SMB (2020) Metal organic framework–derived core-shell CuO@NiO nanosphares as hole transport material in perovskite solar cell. J Solid State Electrochem 24(6):1427–1438. https://doi.org/10.1007/s10008-020-04643-w
120. Zhou X, Qiu L, Fan R, Zhang J, Hao S, Yang Y (2020) Heterojunction incorporating perovskite and microporous metal–organic framework nanocrystals for efficient and stable solar cells. Nanomicro Lett 12(1):80. https://doi.org/10.1007/s40820-020-00417-1
121. Chang C-Y, Wu K-H, Chang C-Y, Guo R-F, Li G-L, Wang C-Y (2022) Enhanced performance and stability of low-bandgap mixed lead–tin halide perovskite photovoltaic solar cells and photodetectors *via* defect passivation with UiO-66-NH_2 metal–organic frameworks and interfacial engineering. Mol Syst Des Eng 7(9):1073–1084. https://doi.org/10.1039/D2ME00032F
122. Lee C-C, Chen C-I, Liao Y-T, Wu KC-W, Chueh C-C (2019) Enhancing efficiency and stability of photovoltaic cells by using perovskite/Zr-MOF heterojunction including bilayer and hybrid structures. Adv Sci 6(5):1801715. https://doi.org/10.1002/advs.201801715
123. Heo DY, Lee TH, Iwan A, Kavan L, Omatova M, Majkova E, Kamarás K, Jang HW, Kim SY (2020) Effect of lead thiocyanate ions on performance of tin-based perovskite solar cells. J Power Sources 458:228067. https://doi.org/10.1016/j.jpowsour.2020.228067
124. Lin Y, Shen L, Dai J, Deng Y, Wu Y, Bai Y, Zheng X, Wang J, Fang Y, Wei H, Ma W, Zeng XC, Zhan X, Huang J (2017) Π-conjugated Lewis base: efficient trap-passivation and charge-extraction for hybrid perovskite solar cells. Adv Mater 29(7):1604545. https://doi.org/10.1002/adma.201604545
125. Niu T, Lu J, Munir R, Li J, Barrit D, Zhang X, Hu H, Yang Z, Amassian A, Zhao K, Liu S (Frank) (2018) Stable high-performance perovskite solar cells via grain boundary passivation. Adv Mater 30(16):1706576. https://doi.org/10.1002/adma.201706576
126. Noel NK, Abate A, Stranks SD, Parrott ES, Burlakov VM, Goriely A, Snaith HJ (2014) Enhanced photoluminescence and solar cell performance *via* Lewis base passivation of organic–inorganic lead halide perovskites. ACS Nano 8(10):9815–9821. https://doi.org/10.1021/nn5036476
127. Qin P-L, Yang G, Ren Z, Cheung SH, So SK, Chen L, Hao J, Hou J, Li G (2018) Stable and efficient organo-metal halide hybrid perovskite solar cells via π-conjugated Lewis base polymer induced trap passivation and charge extraction. Adv Mater 30(12):1706126. https://doi.org/10.1002/adma.201706126
128. Wang S, Ma Z, Liu B, Wu W, Zhu Y, Ma R, Wang C (2018) High-performance perovskite solar cells with large grain-size obtained by using the Lewis acid-base adduct of thiourea. Solar RRL 2(6):1800034. https://doi.org/10.1002/solr.201800034
129. Wang Y, Wu T, Barbaud J, Kong W, Cui D, Chen H, Yang X, Han L (2019) Stabilizing heterostructures of soft perovskite semiconductors. Science (1979) 365(6454):687–691. https://doi.org/10.1126/science.aax8018
130. Wang S, Wang A, Deng X, Xie L, Xiao A, Li C, Xiang Y, Li T, Ding L, Hao F (2020) Lewis acid/base approach for efficacious defect passivation in perovskite solar cells. J Mater Chem A Mater 8(25):12201–12225. https://doi.org/10.1039/D0TA03957H
131. Kim M, Motti SG, Sorrentino R, Petrozza A (2018) Enhanced solar cell stability by hygroscopic polymer passivation of metal halide perovskite thin film. Energy Environ Sci 11(9):2609–2619. https://doi.org/10.1039/C8EE01101J
132. Liu Y, Akin S, Pan L, Uchida R, Arora N, Milić JV, Hinderhofer A, Schreiber F, Uhl AR, Zakeeruddin SM, Hagfeldt A, Dar MI, Grätzel M (2019) Ultrahydrophobic 3D/2D fluoroarene bilayer-based water-resistant perovskite solar cells with efficiencies

exceeding 22%. Sci Adv 5(6):eaaw2543. https://doi.org/10.1126/sciadv.aaw2543
133. Wu WQ, Yang Z, Rudd PN, Shao Y, Dai X, Wei H, Zhao J, Fang Y, Wang Q, Liu Y, Deng Y, Xiao X, Feng Y, Huang J (2019) Bilateral alkylamine for suppressing charge recombination and improving stability in blade-coated perovskite solar cells. Sci Adv 5(3):eaav8925. https://doi.org/10.1126/sciadv.aav8925
134. Zhao Y, Zhou W, Ma W, Meng S, Li H, Wei J, Fu R, Liu K, Yu D, Zhao Q (2016) Correlations between immobilizing ions and suppressing hysteresis in perovskite solar cells. ACS Energy Lett 1(1):266–272. https://doi.org/10.1021/acsenergylett.6b00060
135. Wang K, Liu C, Du P, Zheng J, Gong X (2015) Bulk heterojunction perovskite hybrid solar cells with large fill factor. Energy Environ Sci 8(4):1245–1255. https://doi.org/10.1039/C5EE00222B
136. Peng J, Wu Y, Ye W, Jacobs DA, Shen H, Fu X, Wan Y, Duong T, Wu N, Barugkin C, Nguyen HT, Zhong D, Li J, Lu T, Liu Y, Lockrey MN, Weber KJ, Catchpole KR, White TP (2017) Interface passivation using ultrathin polymer–fullerene films for high-efficiency perovskite solar cells with negligible hysteresis. Energy Environ Sci 10(8):1792–1800. https://doi.org/10.1039/C7EE01096F
137. Liu K, Chen S, Wu J, Zhang H, Qin M, Lu X, Tu Y, Meng Q, Zhan X (2018) Fullerene derivative anchored SnO_2 for high-performance perovskite solar cells. Energy Environ Sci 11(12):3463–3471. https://doi.org/10.1039/C8EE02172D
138. Zuo C, Vak D, Angmo D, Ding L, Gao M (2018) One-step roll-to-roll air processed high efficiency perovskite solar cells. Nano Energy 46:185–192. https://doi.org/10.1016/j.nanoen.2018.01.037
139. Zheng X, Deng Y, Chen B, Wei H, Xiao X, Fang Y, Lin Y, Yu Z, Liu Y, Wang Q, Huang J (2018) Dual functions of crystallization control and defect passivation enabled by sulfonic zwitterions for stable and efficient perovskite solar cells. Adv Mater 30(52):1803428. https://doi.org/10.1002/adma.201803428
140. Zhang S, Wu S, Chen W, Zhu H, Xiong Z, Yang Z, Chen C, Chen R, Han L, Chen W (2018) Solvent engineering for efficient inverted perovskite solar cells based on inorganic CsPbI2Br light absorber. Mater Today Energy 8:125–133. https://doi.org/10.1016/j.mtener.2018.03.006
141. Deng X, Xie L, Wang S, Li C, Wang A, Yuan Y, Cao Z, Li T, Ding L, Hao F (2020) Ionic liquids engineering for high-efficiency and stable perovskite solar cells. Chem Eng J 398:125594. https://doi.org/10.1016/j.cej.2020.125594
142. Shahiduzzaman Md, Yamamoto K, Furumoto Y, Yonezawa K, Hamada K, Kuroda K, Ninomiya K, Karakawa M, Kuwabara T, Takahashi K, Takahashi K, Taima T (2017) Viscosity effect of ionic liquid-assisted controlled growth of CH3NH3PbI3 nanoparticle-based planar perovskite solar cells. Org Electron 48:147–153. https://doi.org/10.1016/j.orgel.2017.06.001
143. Shahiduzzaman M, Yamamoto K, Furumoto Y, Kuwabara T, Takahashi K, Taima T (2015) Ionic liquid-assisted growth of methylammonium lead iodide spherical nanoparticles by a simple spin-coating method and photovoltaic properties of perovskite solar cells. RSC Adv 5(95):77495–77500. https://doi.org/10.1039/C5RA08102E
144. Salado M, Ramos FJ, Manzanares VM, Gao P, Nazeeruddin MK, Dyson PJ, Ahmad S (2016) Extending the lifetime of perovskite solar cells using a perfluorinated dopant. Chemsuschem 9(18):2708–2714. https://doi.org/10.1002/cssc.201601030
145. Bai S, Da P, Li C, Wang Z, Yuan Z, Fu F, Kawecki M, Liu X, Sakai N, Wang JT-W, Huettner S, Buecheler S, Fahlman M, Gao F, Snaith HJ (2019) Planar perovskite solar cells with long-term stability using ionic liquid additives. Nature 571(7764):245–250. https://doi.org/10.1038/s41586-019-1357-2
146. Lu H, Krishna A, Zakeeruddin SM, Grätzel M, Hagfeldt A (2020) Compositional and interface engineering of organic-inorganic lead halide perovskite solar cells. iScience 23(8):101359. https://doi.org/10.1016/j.isci.2020.101359
147. Zhang H, Wu Y, Shen C, Li E, Yan C, Zhang W, Tian H, Han L, Zhu W (2019) Efficient and stable chemical passivation on perovskite surface via bidentate anchoring. Adv Energy Mater 9(13):1803573. https://doi.org/10.1002/aenm.201803573
148. Qi W, Zhou X, Li J, Cheng J, Li Y, Ko MJ, Zhao Y, Zhang X (2020) Inorganic material passivation of defects toward efficient perovskite solar cells. Sci Bull (Beijing) 65(23):2022–2032. https://doi.org/10.1016/j.scib.2020.07.017
149. Chen C, Li F, Zhu L, Shen Z, Weng Y, Lou Q, Tan F, Yue G, Huang Q, Wang M (2020) Efficient and stable perovskite solar cells thanks to dual functions of oleyl amine-coated $PbSO_4(PbO)_4$ quantum dots: defect passivation and moisture/oxygen blocking. Nano Energy 68:104313. https://doi.org/10.1016/j.nanoen.2019.104313
150. Yang S, Chen S, Mosconi E, Fang Y, Xiao X, Wang C, Zhou Y, Yu Z, Zhao J, Gao Y, De Angelis F, Huang J (2019) Stabilizing halide perovskite surfaces for solar cell operation with wide-bandgap lead oxysalts. Science (1979) 365(6452):473–478. https://doi.org/10.1126/science.aax3294
151. Wang Z, Wu T, Xiao L, Qin P, Yu X, Ma L, Xiong L, Li H, Chen X, Wang Z, Wu T, Xiao ML, Qin P, Yu DX, Ma DL, Xiong DL, Li DH, Chen X (2021) Multifunctional potassium hexafluorophosphate passivate interface defects for high efficiency perovskite solar cells. J Power Sources 488:229451. https://doi.org/10.1016/j.jpowsour.2021.229451
152. Bi H, Liu B, He D, Bai L, Wang W, Zang Z, Chen J (2021) Interfacial defect passivation and stress release by multifunctional KPF_6 modification for planar perovskite solar cells with enhanced efficiency and stability. Chem Eng J 418:129375. https://doi.org/10.1016/j.cej.2021.129375
153. Gong X, Guan L, Pan H, Sun Q, Zhao X, Li H, Pan H, Shen Y, Shao Y, Sun L, Cui Z, Ding L, Wang M (2018) Highly efficient perovskite solar cells via nickel passivation. Adv Funct Mater 28(50):1804286. https://doi.org/10.1002/adfm.201804286
154. Wu W-Q, Rudd PN, Ni Z, Van Brackle CH, Wei H, Wang Q, Ecker BR, Gao Y, Huang J (2020) Reducing surface halide deficiency for efficient and stable iodide-based perovskite solar cells. J Am Chem Soc 142(8):3989–3996. https://doi.org/10.1021/jacs.9b13418
155. Chen H, Liu T, Zhou P, Li S, Ren J, He H, Wang J, Wang N, Guo S (2020) Efficient bifacial passivation with crosslinked thioctic acid for high-performance methylammonium lead iodide perovskite solar cells. Adv Mater 32(6):1905661. https://doi.org/10.1002/adma.201905661
156. Xie L, Zhang T, Zhao Y (2020) Stabilizing the MAPbI3 perovksite via the in-situ formed lead sulfide layer for efficient and robust solar cells. J Energy Chem 47:62–65. https://doi.org/10.1016/j.jechem.2019.11.023
157. Son D-Y, Kim S-G, Seo J-Y, Lee S-H, Shin H, Lee D, Park N-G (2018) Universal approach toward hysteresis-free perovskite solar cell via defect engineering. J Am Chem Soc 140(4):1358–1364. https://doi.org/10.1021/jacs.7b10430
158. Li C, Wang A, Xie L, Deng X, Liao K, Yang J, Li T, Hao F (2019) Emerging alkali metal ion (Li^+, Na^+, K^+ and Rb^+) doped perovskite films for efficient solar cells: recent advances and prospects. J Mater Chem A Mater 7(42):24150–24163. https://doi.org/10.1039/C9TA08130E
159. Yuan S, Qian F, Yang S, Cai Y, Wang Q, Sun J, Liu Z, Liu S (Frank) (2019) NbF 5: a novel A-phase stabilizer for FA-based perovskite solar cells with high efficiency. Adv Funct Mater 29(47):1807850. https://doi.org/10.1002/adfm.201807850

160. Lu J, Chen S-C, Zheng Q (2019) Defect passivation of CsPbI2Br perovskites through Zn(II) doping: toward efficient and stable solar cells. Sci China Chem 62(8):1044–1050. https://doi.org/10.1007/s11426-019-9486-0
161. Li H, Shi J, Deng J, Chen Z, Li Y, Zhao W, Wu J, Wu H, Luo Y, Li D, Meng Q (2020) Intermolecular π–π conjugation self-assembly to stabilize surface passivation of highly efficient perovskite solar cells. Adv Mater 32(23):1907396. https://doi.org/10.1002/adma.201907396
162. Shao J, Yang S, Liu Y (2017) Efficient bulk heterojunction $CH_3NH_3PbI_3$–TiO_2 solar cells with TiO_2 nanoparticles at grain boundaries of perovskite by multi-cycle-coating strategy. ACS Appl Mater Interfaces 9(19):16202–16214. https://doi.org/10.1021/acsami.7b02323
163. Cao J, Li C, Lv X, Feng X, Meng R, Wu Y, Tang Y (2018) Efficient grain boundary suture by low-cost tetra-ammonium zinc phthalocyanine for stable perovskite solar cells with expanded photoresponse. J Am Chem Soc 140(37):11577–11580. https://doi.org/10.1021/jacs.8b07025